Fluorescence Based Detection of Magnetic Field Effect on Photolyases and Flavin Containing Solutions

by

Gamze Gül

A Dissertation Submitted to the
Graduate School of Sciences and Engineering
in Partial Fulfillment of the Requirements for
the Degree of

Master of Science

in

Physics

KOÇ
UNIVERSITY

August 21, 2019

Fluorescence Based Detection of Magnetic Field Effect on Photolyases and Flavin Containing Solutions

Koç University

Graduate School of Sciences and Engineering

This is to certify that I have examined this copy of a master's thesis by

Gamze Gül

and have found that it is complete and satisfactory in all respects,
and that any and all revisions required by the final
examining committee have been made.

Committee Members:

_____

Prof. Alper Kiraz

_____

Prof. Ataç İmamoğlu

_____

Prof. İ. Halil Kavaklı

_____

Asst. Prof. Serap Aksu Ramazanoğlu

_____

Asst. Prof. Ahmet Erten

Date: _____

To my mother,

ABSTRACT

It has been known that bird's navigation mechanism relies on the geomagnetic field; however, the primary sensor is still a matter of debate. One of the leading hypotheses is based on the magnetic sensitivity of the radical pairs. According to this model, inside the photoactivated proteins such as cryptochrome and photolyase, flavin-tryptophan radical pairs are formed by photon absorption and electron transfer, and they can undergo coherent singlet-triplet interconversion which is affected by an external magnetic field.

Absorption spectroscopy has been predominantly employed to monitor such magnetic field effects. This technique requires relatively high sample concentrations. Moreover, magnetic field sensitivity of individual molecules with different orientations is lost and only an average magnetoreception behavior can be observed. Recently, fluorescence-based approach has emerged as an alternative experimental strategy which is generally easier to perform and more sensitive. Despite this, up to now fluorescence-based experiments only revealed the magnetic field effect in solutions containing flavin and tryptophan, but not actual photoactivated proteins.

In this thesis, the magnetic field effect on flavin containing solutions and photolyases is detected by utilizing fluorescence-based experiments. In the presence of around 28 mT magnetic field, up to -5.55% magnetic field effect is observed for the solution of 1 μM flavin adenine dinucleotide (FAD) and 300 μM Trp. The roles of laser intensity, pH of the buffer, and magnetic field strength in the magnetic field sensitivity are investigated for the FAD and Trp containing solutions. The fluorescence based experiments are also conducted with photolyases. -1.34% and -1.01% magnetic field effects are measured for the solutions of 170 μM *Vibrio cholerae* photolyase (VcPHR) and 166 μM *Escherichia coli* photolyase (EcPHR) respectively. Moreover, simulations

to understand quantum coherence in the radical pair mechanism are performed, and the fluorescence based observation of coherent interconversion is discussed. Finally, we suggest conjugating the photoexcited proteins or flavin with dye molecules which serve as acceptors in Förster resonance energy transfer (FRET). In this method, the decay rate of the singlet and triplet states is further enhanced, revealing higher sensitivity of magnetic field effect.

ÖZETÇE

Kuşların yön bulma mekanizmalarının dünyanın manyetik alanına bağlı olduğu bilinse de, birincil sensörün ne olduğu hala bir tartışma konusudur. Bu konuda başta gelen hipotezlerin biri radikal çiftlerinin manyetik alana karşı duyarlılığına dayanmaktadır. Bu modele göre, cryptochrome ya da photolyase gibi fotoaktive proteinlerin içinde, foton soğurulması ve elektron transferi ile flavin-tryptophan (Trp) radikal çiftleri oluşturulabilir. Oluşan bu radikal çiftlerini tekli ve üçlü (singlet ve triplet) durumlar arasında dışarıdaki bir manyetik alana duyarlı koherent bir döngüye girerler.

Manyetik alan etkisini gözlemlemek için ağırlıklı olarak soğurma (absorbsiyon) spektroskopisi kullanılabilir. Fakat bu teknik örneklerin yüksek konsantrasyona sahip olmasını gerektirir. Buna ek olarak, farklı oryantasyona sahip moleküllerin manyetik alana verdiği tepki tek tek ölçülemez, sadece bu tepkilerin ortalaması gözlemlenebilir. Son zamanlarda soğurma spektroskopisine alternatif olarak floresan temelli bir yaklaşım ortaya konuldu. Bu metot daha hassas ölçümler yapabilir ve deneysel olarak gerçekleştirilmesi daha kolaydır.

Bu tezde, manyetik alanın flavin molekülu içeren çözeltilerdeki ve photolyase proteini üzerindeki etkisini floresan bazlı deneyler kullanarak saptandı. 28 mT manyetik alan varlığında, 1 μM flavin adenine dinucleotide (FAD) ve 300 μM Trp içeren çözeltilerin -%5.5 e varan manyetik alan etkisi gösterdiğini gördük. Bu çözeltiler kullanılarak çözeltinin pH değeri, lazer gücü ve manyetik alanin gücü gibi parametrelerin manyetik alana karşı duyarlılıktakı rölü araştırıldı. Floresan bazlı deneyler, protein çözeltileri için de yürütüldü. 170 μM *Vibrio cholerae* photolyase (VcPHR) ve 166 μM *Escherichia coli* photolyase (EcPHR) için sırasıyla -%1.34 ve -%1.01 manyetik alan etkisi ölçüldü. Buna ek olarak, kuantum koherensi anlamak için simulasyonlar yapıldı ve bu konseptin floresan bazlı deneyler ile gözlemlenmesi tartışıldı. Son olarak, flore-

san bazlı deneylere bir gelizştirme olarak fotoaktive proteinlere ve flavin molekülüne boya bağlamayı önerdik. Förster rezonans enerji transferi (FRET) olarak bilinen bu teknikte boya molekülleri alıcı olarak davranırlar. Boylece tekli ve üçlü durumların azalım hızı arttırılarak, manyetik alan etkisi daha yüksek hassaslıkta gözlemlenebilir.

ACKNOWLEDGMENTS

I would like to begin by thanking my advisor, Prof. Alper Kiraz, for his continuous encouragement and support over two years. He has provided a great environment and resources to express my ideas and develop this research. I would also like to express my gratitude to my coadvisor, Prof. Atac Imamoglu, for his valuable supervision. He has showed different point of views to widen this study. I am also grateful that their guidance was not only limited by my thesis project, but also they have contributed to my personal and professional development as a scientist.

I would like to thank Adnan Kurt for his design of MagnaPulsa. The experiments presented in this thesis would not have been possible without his great knowledge and help. I also greatly acknowledge Prof. Halil Kavakli and his group members for being in a close collabration about the proteins. My grateful thanks are also extended to Prof. Alphan Sennaroglu, for sharing his knowledge in the photonics courses and also for providing me with an excellent assitantship environment to enhance my skills in teaching. I would like to thank Prof. M. Ozgur Oktel and Prof. Orhan Arikan for contributing to my academic career with their experiences and knowledge during my undergraduate years in Bilkent.

I would also like to thank Nima Bavili in particular who very patiently taught me many critical aspects of experimental optics, and I am also grateful for the proof reading of this thesis. I would like to acknowledge all the former and current members of our research group for creating an fruitful environment and helping me in the experimental setup.

Thanks to my oldest friend Yiğit Karakaş who has inspired me with his unique designs since 2000. I also would like to thank Ekin Ulusoy, Demet Candemir, Tuğçe Banyocu, Ozan Karakuz and Yılmaz Genç for being excellent friends and for encour-

aging me throughtout my academic career.

The support and understanding of my family was essential to complete this thesis. I would especially like to thank the next generation of our family: Büşra, Betül, Çağatay and Toprak. Finally, I would like to express my heartedly thanks to my mother, Sahibe, for her continued encouragement. This thesis is dedicated to her.

TABLE OF CONTENTS

LIST OF TABLES

LIST OF FIGURES

NOMENCLATURE

AtCRY	*Arabidopsis thaliana* cryptochrome
CW	Continuous wave
EcPHR	*Escherichia coli* photolyase
DmCRY1	*Drosophila melanogaster* cryptochrome
emCCD	Electron-multiplying charged coupled device
FAD	Flavin adenine dinucleotide
FFT	Fast Fourier transform
FMN	Flavin mononucleotide
FRET	Förster resonance energy transfer
ISC	Intersystem crossing
MF	Magnetic field
MFE	Magnetic field effect
MTHF	Methylene tetrahydrofolate
NHS	N-Hydroxysuccinimide
RP	Radical pair
RPM	Radical pair mechanism
Trp	Tryptophan
UV-vis	Ultraviolet-visible
VcCRY1	*Vibrio cholerae* cryptochrome
VcPHR	*Vibrio cholerae* photolyase

Chapter 1

INTRODUCTION

1.1 Overview

The interaction with magnetic fields has been utilized to develop new technologies for several years such as sensory systems [1], and imaging techniques [2]. However, we can poorly understand natural processes that are affected by the magnetic field [3]. In recent decades, the research on effects of low magnetic fields on biological systems have gained importance. For instance, there has been proposed a mechanism to uncover the association between childhood leukaemia and high voltage lines which produces magnetic fields in the range of μT at 50/60 Hz [4, 5].

Another example of the interaction between magnetic fields and biological systems is magnetoreception. Magnetoreceptors are the magnetic sensors of organism such as plants [6], some sea animals [7, 8, 9], mammals [10, 11], and birds [12]. They utilize this system for several reasons, for example migration of birds. In addition to the inherently obtained migration routes, these birds need a compass system [13, 14].

The compass system of migratory birds has been under investigation for many years. The role of the geomagnetic field in the sensory system was proposed by Wiltschko [15, 16, 17], since then, several experiments on birds have been conducted to reveal the dependants of the mechanism.

Further research demonstrated that migratory birds utilize the inclination of the geomagnetic field instead of polarity information in order to generate a map of their routes [17, 18]. Moreover, the experiments on European robins showed that the navigation system of migratory birds performs better at lower wavelength lights as

shown in Figure 1.1 [19].

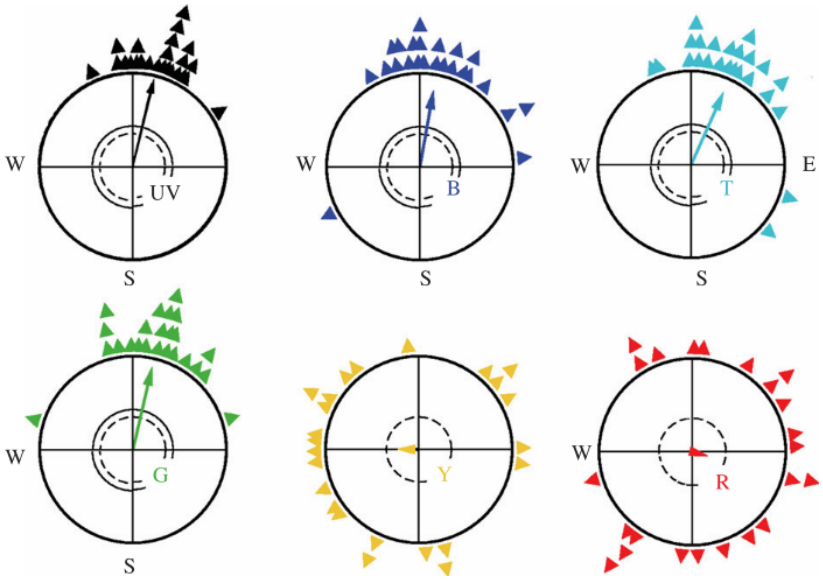

Figure 1.1: Experiments on European robins in different illumination conditions. Smaller arrows on the outer edges of the circles show the flying directions of individual birds. The arrow at the center represents the average of all the directions. The colors of arrows indicate the ambient light [19]

Over the years, two hypothesises have been built to explain the avian magnetic compass: magnetite based and radical pair based magnetoreception. Although this thesis focuses on detection of the radical pair based magnetoreception, we should discuss both hypothesises starting from the older one.

1.1.1 The Magnetite Particle Hypothesis

Magnetite is a iron-oxide crystal (Fe_2O_3) which can be found in the form of crystal particles. Particles in the size of ∼50 nm can have permanent magnetic moment which can be aligned with respect to the geomagnetic field by rotation [20, 21, 22]. If particles are as small as 20 nm, they become superparamagnetic [21]. They can move because of the attraction or repulsion by other particles. Therefore, magnetite based hypothesis requires a mechanical sensor close to the particles so that the animal can transmit magnetic information [23].

Existence of Fe_2O_3 is proved for some animals such as worms and some bacterias [17, 24, 25]. However, the existence does not indicate the magnetoreception or any detection system [25]. The particles must have specifically located so that it can be related to a specific operation in the body. Moreover, this system must be linked to the neural system [25, 26, 27]. To illustrate, the magnetotactic bacteria have ability to synthesize magnetite particles which leads to the orientation with the geomagnetic field; however, this orientation is rather passive. There is no active magnetoreception system involved in the orientation. Although this result does not demonstrate the magnetoreception, it implies that the magnitite particle can be produced by the organism [17, 25].

The closest thing to a magnetoreception is a nerve in a birds's upper beak which contains iron minerals. The opthalmic branch of trigeminal nerve, V1, is proposed as a magnetic map sensor for migratory birds [28]. V1 might be responsible for the transmission of location information to the brain [29]. In conclusion, although the research have considered that V1 can play role in the magnetic sensory system, the mechanism is still undetermined.

1.1.2 The Radical Pair Mechanism

This hypothesis relies on the generation of radical pairs which can be sensitive to magnetic field [30]. The requirement of the radical pair based compass system is the change in the output of the reaction with respect to the direction of the geomagnetic field [14]. However, this requirement is apparently hard to satisfy considering the thermal energy level of molecules (k_BT). The Earth's magnetic field ($\sim$50 μT) cannot cause an interaction even comparable with the thermal energy of molecules. However, once the radical pairs have sufficient energy by photoexcitation, they reach the state away from equilibrium, and sensitive to small magnetic field changes [14].

After this idea was proposed [31], scientists verified it experimentally by showing that radical pairs can react to magnetic field in mT range [32, 33, 34]. Moreover, the experiments on the migratory birds suggested the light dependence of the compass

system [35]. Although the agreement of these experimental studies with the theory promoted the radical pair based model, it was unknown that whether the radical pairs are the magnetoreceptors because of three reasons: First, there was no solid evidence that weaker magnetic fields (μT) have an impact on the radical pairs, second, the molecule which should contain these radicals was uncovered, and the third, it was unknown how the output of chemical reaction is transmitted to the brain of the animal [14].

Even though first criticism is still valid for the radical pair mechanism, recently, several models for the transmission of the signal have been proposed [36, 37]. More importantly, the candidate molecule has been suggested with a lot of strong arguments. This molecule called cryptochrome is explained in the following section.

1.1.3 The Candidate Molecules

After successfully explaining the magnetic field sensing by the radical pair mechanism, the responsible molecule has been investigated for the magnetic compass system in the animal's body [38]. The strongest candidate has been cryptochrome with its ability to absorb blue light [39, 40, 41, 42, 43] and its presence in the eye of migratory birds [44, 45, 46].

Cryptochromes are similar to photlyases, and both of them are called flavoproteins since they contains FAD cofactor which is the blue light absorber [42]. In cryptochromes, tryptophan triad (or chain) is located close to the FAD molecule (Figure 1.2) that allows rapid transfer of electrons [47, 48]. This provides photolyases the capability of DNA repair after UV-damage [43]. For crytochromes, it results in the genration of radical pairs [49].

Thus far, the *in vitro* experiments showing the magnetic sensibility of cryptochromes and photolyases became the most convincing evidence of the radical pair based magnetoreception. Studies on *Escherichia coli* photolyase (EcPHR) and *Arabidopsis thaliana* cryptochrome (AtCRY) exhibited response to the magnetic field in mT level [50, 51]. Moreover, *Drosophila melanogaster* cryptochrome (DmCRY)

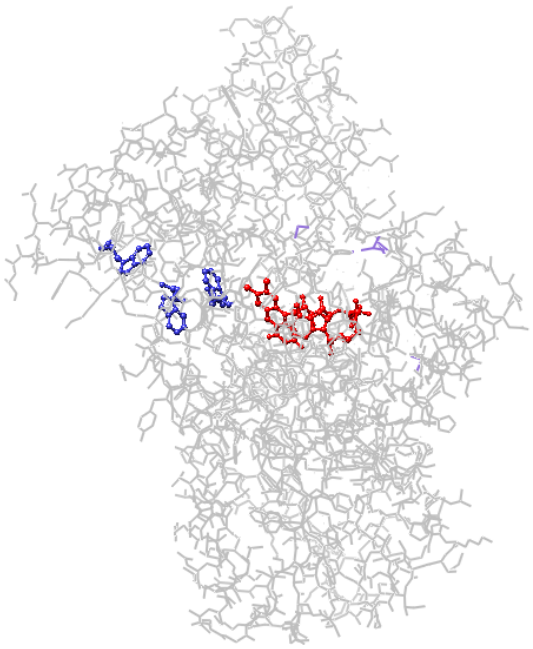

Figure 1.2: FAD(red) and Trp-triad(blue) inside a *Arabidopsis thaliana* cryptochrome (AtCRY) molecule (PDB code:1u3d)

which is an animal cryptochrome (fruit fly) was investigated [52]. However, the effect of lower magnetic fields such as geomagnetic field is not observed for flavoproteins yet. Therefore, further reseacrh is needed for the lower wavelength, and also for other alternatives as a magnetoreceptor molecule.

1.2 Scope of the Thesis

This thesis aims to improve the existing methods to understand the mechanism under the magnetic sensitivity of flavin containing solutions and flavoproteins in more detail. In order to decide our direction, the theoretical background is given in the next chapter starting from the definition of spin to the quantum coherence.

Chapter 3 discusses the quantum coherence in radical pair chemistry thoroughly. the rate equation which interprets the reaction dynamics is simulated. The simulation results is investigated to determine the requirements of an experiment which enables

us observing quantum coherence by fluorescence data.

In Chapter 4, the fluorescence based observation techniques is introduced. The magnetic field effect on flavin containing solutions is observed by utilizing these techniques. The reaction scheme is analysed by varying several parameters in the experiments such as the presence of donor molecule in the solution, pH of the buffer, laser intensity, and magnetic field strength. Although this chapter is important to collect evidences for the radical pair mechanism, flavin containing solutions are different from the flavoproteins in some aspects.

Therefore, Chapter 5 is dedicated to crytochromes and photolyases. The reaction scheme which is dissimilar from the the reaction scheme of flavin containing solutions is discussed. The differences between the literature and our work are addressed.

The FRET enhancement to our fluorescence based techniques is proposed in Chapter 6. The requirements for a dye conjugation is studied. Moreover, the modification in the reaction schemes is debated.

In the final chapter, the results of the simulations and experiments are summarized. The existing challenges and the possible solutions are reported. The future directions for some areas are suggested.

Chapter 2

THEORETICAL BACKGROUND

2.1 Spin

Spin is the angular momentum that particles have intrinsically in addition to the angular momentum due to their orbital motion. Dirac developed this concept and there is no classical analogue for it.

Spin is defined by the vector, **s**, and it is associated with a spin quantum number s. The projection of the vector on of the axis is represented by $m_s = s, s-1, ..., -s$. Unlike the classical angular momentum, spin quantum number can take half integer values. Fermions (protons, neutrons, and electrons) are the particles with spin quantum number of $s = 1/2$ whereas bosons such as photon have $s = 0, 1, 2, ...$. The amplitude of a spin vector ($\mathbf{S^2}$) and the projection of it in the z-axis ($\mathbf{S_z}$) can be calculated as follows:

$$\mathbf{S^2}\,|s, m_s\rangle = \hbar^2 s(s+1)\,|s, m_s\rangle \tag{2.1}$$

$$\mathbf{S_z}\,|s, m_s\rangle = m_s\hbar\,|s, m_s\rangle \tag{2.2}$$

For an electron, s is 1/2 and allowed values of m_s is turned out to be 1/2 or -1/2. $m_s = 1/2$ state is known as up state ($|\uparrow\rangle$ or $|\alpha\rangle$), and $m_s = -1/2$ state is denoted as down state ($|\downarrow\rangle$ or $|\beta\rangle$).

$$\mathbf{S^2}\,|\uparrow\rangle = 3\hbar^2/4\,|s, m_s\rangle \qquad \mathbf{S_z}\,|\uparrow\rangle = \hbar/2\,|s, m_s\rangle \tag{2.3}$$

$$\mathbf{S^2}\,|\downarrow\rangle = 3\hbar^2/4\,|s, m_s\rangle \qquad \mathbf{S_z}\,|\downarrow\rangle = -\hbar/2\,|s, m_s\rangle \tag{2.4}$$

Therefore, an electron can possess two orientations which are energetically degenerate if there is no magnetic field. Moreover, it is crucial to learn coupled spin states to understand radical pair chemistry.

A system with two unpaired electrons have total spin quantum number which can be calculated as a summation of individual spins. The possible values for the total spin quantum number can be represented as a Clebsh-Gordan series:

$$\mathbf{S} = \mathbf{s_1} + \mathbf{s_2} = (s_1 + s_2), (s_1 + s_2 - 1)... |s_1 - s_2| \tag{2.5}$$

Since the spin quantum number of a single electron is 1/2, total spin quantum number can be either 0 or 1 for an electron pair. s = 0 state is called the singlet state, the projection of it on the z-axis must be 0. On the other hand, s = 1 results in three different projectionon the z-axis represented by $m_s = 1, 0, -1$. therefore, they are called the triplet states.

$$|S\rangle = \frac{1}{\sqrt{2}}(|\uparrow\downarrow\rangle - |\downarrow\uparrow\rangle) \tag{2.6}$$

$$|T_-\rangle = |\downarrow\downarrow\rangle \tag{2.7}$$

$$|T_0\rangle = \frac{1}{\sqrt{2}}(|\uparrow\downarrow\rangle + |\downarrow\uparrow\rangle) \tag{2.8}$$

$$|T_+\rangle = |\uparrow\uparrow\rangle \tag{2.9}$$

Coupled spins play important roles in several phenomena which allow radical pairs to sense magnetic fields. Before investigating these phenomena, it is necessary to analyse interactions of coupled spins with their environment.

2.2 Interactions

2.2.1 The Zeeman Effect

Electrons behave like magnetic dipoles due to their spins, and they can interact with the external magnetic field. This phenomenon known as the Zeeman effect [53]. The Hamiltonian can be written as:

$$\hat{H} = -\hat{\mu}_{\mathbf{s}} \cdot \mathbf{B} \tag{2.10}$$

Electron spin quantum number is related to magnetic moment by,

$$\hat{\mu}_{\mathbf{s}} = \frac{g_e \mu_B}{\hbar}\mathbf{s} \tag{2.11}$$

where g_e is the electron g-factor,and μ_B is the Bohr magneton:

$$\mu_B = \frac{e\hbar}{2m_e}. \tag{2.12}$$

in which e is the charge of the electron, m_e is the mass of the electron, and $\hbar$ is the Planck constant. the magnetic dipole moment and the gyromagnetic ratio of the electron are also related by $\mu_B = -\frac{\gamma_e \hbar}{g_e}$. Therefore, we know the ratio of angular momentum to spin angular momentum of the electron by [54]:

$$\gamma_e = \frac{g_e e}{2m_e} \tag{2.13}$$

Assume that we take only z-component of the spin vector into consideration, then:

$$\mu_z = -\gamma_e \mu_B m_s \hbar \tag{2.14}$$

Therefore, the energy splitting can be calculated according to:

$$E = -\gamma_e m_s \hbar B = g_e \mu_B m_s B \tag{2.15}$$

Two different orientations of spin vector in the z-axis lead to the splitting of energy levels as shown in Figure 2.1.

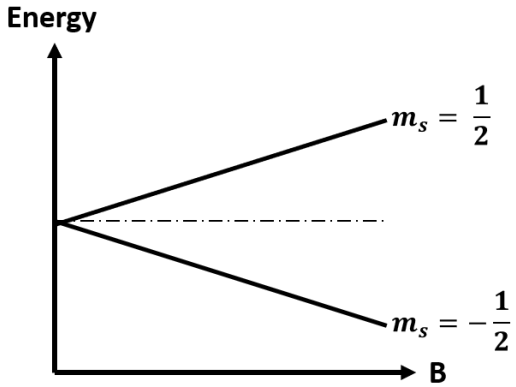

Figure 2.1: Energy splitting due to the external magnetic field for a spin-1/2 particle

The difference in the energy levels is proportional to the strength of external magnetic field.

$$\Delta E = g_e \mu_B B \tag{2.16}$$

This interaction oscillates the direction of spin quantum vector. It can be associated with the frequency called Larmor frequency [14]:

$$\omega_L = \frac{\Delta E}{\hbar} = \frac{g_e \mu_B B}{\hbar} \tag{2.17}$$

For the coupled spins, energy levels split into three with respect to their m_s values in the presence of external magnetic field. Since singlet state and one of the triplet states have $m_s = 0$. They coexist in the same energy level independent from the strength of magnetic field as shown in Figure 2.2.

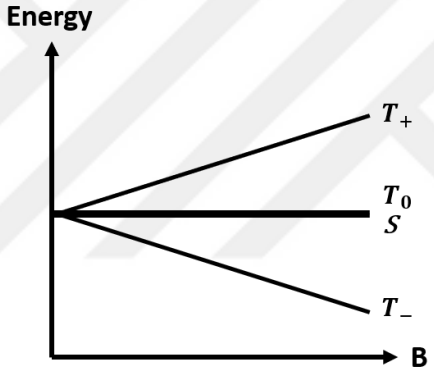

Figure 2.2: Energy splitting due to the external magnetic field for a pair of spin-1/2 particles

However, this plot is only true when there is no other interaction. Therefore, we should also investigate the effect of nuclear spins and electron-electron interactions for more further understanding.

2.2.2 Exchange Coupling

Th exchange interaction describes the effect of two unpaired electrons due to their exchange symmetry. It is related to the Pauli exclusion principle and there is no classical analogue. The exchange interaction can split the energy levels of singlet and triplet states even in the absence of any external magnetic field. The Hamiltonian can be written accordingly as:

$$\hat{H} = -2J(r)\mathbf{s_1} \cdot \mathbf{s_2} \tag{2.18}$$

r represents the distance between radicals, and it determines the energy difference between states. J(r) can be either positive or negative: however, it can be neglected for larger distances (r>1nm) due to the exponential dependence. For smaller intermolecular distance, it prevents singlet-triplet interconversion and magnetic sensitive respectively.

2.2.3 Dipole-Dipole Interaction

The magnetic dipole moment of two unpaired electrons can also interact with each other, and lead to energy level splitting in the triplet states like the Zeeman effect. The Hamiltonian can be formed as:

$$\hat{H} = \mathbf{s_1} \cdot \hat{\mathbf{D}} \cdot \mathbf{s_2} \tag{2.19}$$

D is the tensor which contains the direction of the effect. The dipole-dipole interaction is more effective than the exchange interaction due to the distance dependence. However, it can be negligible for the solutions due to the anisotropy in the interaction.

2.2.4 Hyperfine Interaction

Unpaired electrons also interact with the nuclei of the atoms in radical pairs. This is called hyperfine interaction, and it contains both electrical and magnetic terms. The electrical component is negligible considering the usual distance between electron and nucleus. However, if radical pair contains magnetic nuclei, the hyperfine interaction plays important role in the spin dynamics.

Nuclear spin angular momentum is denoted by I. It can have projection $m_I = -I, -I+1, .., I-1, I$ as other angular momentum numbers. However, it is zero unless there are atoms with odd numbers of protons or neutrons or both. Some isotopes can have magnetic nuclei, hence the natural abundance is also important.

Isotope	Natural Abundance	Number of protons	Number of neutrons	Magnetic Field
^{1}H	**99.985%**	**1**	**0**	**2.44**
^{2}H	0.015%	1	1	0.61
^{12}C	98.892%	6	6	0.00
^{13}C	1.108%	6	7	0.61
^{14}N	**99.63%**	**7**	**7**	**0.29**
^{15}N	0.37%	7	8	0.25
^{16}O	99.8%	8	8	0.00
^{17}O	0.037%	8	9	1.13

Table 2.1: Magnetic features of elements [14]

As shown in Table 2.1, nitrogen and hydrogen have non-zero magnetic moment and almost 100% natural abundance. Organic molecules usually contains them. Therefore, the hyperfine interaction can be added to effective magnetic field as an extra term as:

$$B_{eff} = B + m_I a \tag{2.20}$$

where a is the isotropic hyperfine coupling constant. Since the external magnetic field is the same for the electrons, hyperfine coupling must be different for them. Therefore, they can precess with different Larmor frequencies which results in singlet-triplet interconversion.

2.3 Radical Pair Chemistry

Interaction between two spin angular momentum is not only important for radical pairs, but also crucial to understand the spin conservation or Intersystem crossing which are responsible for the optical properties of molecules such as fluorescence and phosphorescence [55]. To this extent, we should first discuss the mechanism behind spin conservation.

According to the Pauli Exclusion principle, two identical electrons cannot occupy the same quantum states simultaneously. If they are in the same energy levels, their spin wavefunction must be opposite. Thus, we can consider ground state as a singlet state since two electrons have opposite spin states as simply shown in Figure 2.3.

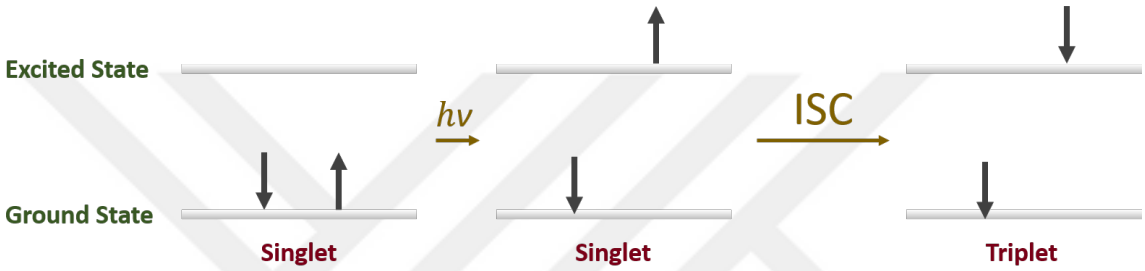

Figure 2.3: Photoexcitation of an atom in a singlet ground state followed by Intersystem crossing (ISC)

If an excited electron is exposed to the interactions discussed above, its spin angular momentum can be distorted. This process can result in triplet excited state, and it is called Intersystem crossing (ISC).

Radical pairs can be singlet born, if photoexcitation of the acceptor molecule is followed by a rapid electron transfer from a donor molecule. On the other hand, a triplet born radical pair can be obtained if ISC is faster than the electron transfer. In any case, radical pair can undergo singlet-triplet interconversion if there is an anisotropic hyperfine interactions. In the absence of any external magnetic field, spin angular momentums precess coherently. It is also called quantum coherence, and it is the heart for the magnetic sensitivity of radical pairs.

On the other hand, the spin angular momentum of excited electrons can be distorted due to the interactions with other electrons or the nuclei. It also breaks the quantum coherence. It is crucial to maintain coherence longer than the lifetime of singlet and triplet states. Therefore, long-lived radical pairs are necessary to sense an external magnetic field.

As a final step, molecules turn back to their ground state spin selectively by a

reverse electron transfer. It can be radiative or non-radiative. The radiative ways are discussed in the following section.

2.4 Fluorescence and Phospherecense

Absorption of a single photon excites the electron to higher energy levels with respect to the wavelength of the photon. If it is excited to the second energy level, it can decay to the first excited state which is called internal conversion. An electron in the first excited energy level can decay to the ground level, and radiate fluorescence. The fluorescence lifetime can vary for different elements; however, it is approximately 10^{-9} seconds. On the other hand, Intersystem crossing can also occur. Since the transition from excited triplet to singlet ground states is not spin-allowed. The radiation lasts longer (10^{-6} s), and it is called phosphorescence.

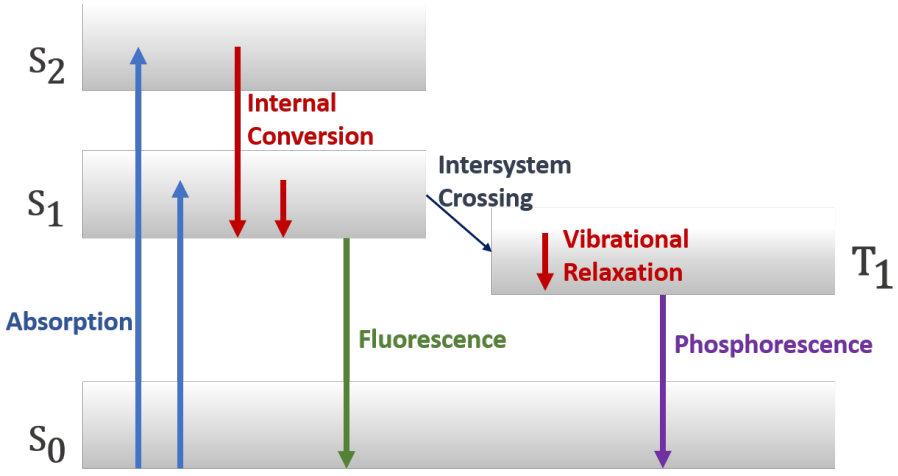

Figure 2.4: Jablonski diagram for fluorescence and phosphorescence

In some cases, molecules can lose their ability to fluoresce permanently. This phenomenon called photobleaching (or fading) caused by the change in spin state of the electron. This results in covalent bond breaking. Therefore, molecule cannot absorb and emit light. Photobleaching rate can vary for molecules.

2.5 Summary

Spin angular momentums of two electrons can interact with each other, and coupled spins are represented with a total spin angular momentum number. According to this number, the energy levels of coupled spins can be modified by an external magnetic field. It is difficult to observe this effect due to the thermal fluctuation. Radical pairs generated by an electron transfer can undergo singlet triplet interconversion.

In the absence of any external magnetic field, the interconversion occurs coherently due to the anisotropic hyperfine interaction. Fortunately, if radical pairs are long-lived, the external magnetic field affects the population of the states, and enables the detection of the magnetic field.

Fluorescence is a preferable signal to probe magnetic field effect. It gives the ground state population under a continuous illumination; however, we should take photobleaching into consideration.

Chapter 3

QUANTUM COHERENCE IN THE RADICAL PAIR MECHANISM

3.1 Overview

Magnetic field sensitivity relies on the interconversion of singlet and triplet states after the radical pairs. In the absence of any external magnetic field, the interconversion occurs coherently due to the interactions discussed in the previous chapter.

The quantum coherence has been investigated indirectly by modifying the reaction schemes by several ways. For example, an external magnetic field is applied to isolate triplet states and break the coherence in the transition. Besides, the properties of solution buffers have been varied systematically to alter the lifetimes of singlet and triplet states. Although the effect of the coherent transition has been illustrated theoretically and experimentally, there has been no research on the demonstration of the quantum coherence in radical pair mechanism directly.

The observation of populations of either singlet or triplet states is challenging because of the degeneracy in their energy levels. However, probing the modulation in the ground state population indicates the change in the singlet state because of spin conservation. Therefore, the fluorescence based techniques to probe ground state population can be employed to observe the quantum coherence in the radical pair model.

In this chapter, we aim to simulate a simplified version of the radical pair mechanism in order to understand the reaction dynamics. Then, we discuss the possible experiments and the required conditions to conduct them.

3.2 Reaction Scheme

Simulation of a complete reaction scheme might be time consuming. Instead, we simplify it by representing some steps such as electron transfer or ISC with a rate constant as you can see in Figure 3.1.

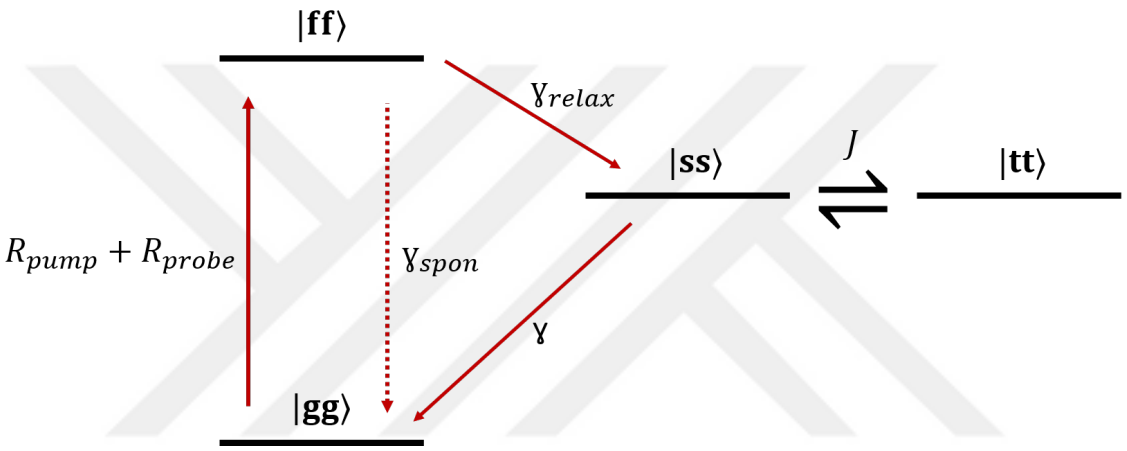

Figure 3.1: Jablonski diagram for the simplified reaction scheme of radical pair mechanism

Photoexcitation of molecules depends on R_{pump} and R_{probe} which we have full control on. Once the molecules are excited with these rates, they can either go back to ground state by emitting fluorescence, or they can form a radical pair with a donor molecule.

In the absence of any external magnetic field, the interconversion between singlet and triplet state is represented with the rate constant J. Molecules can decay back to their ground state via singlet state due to the spin conservation. The non-radiative decay from the triplet state is ignored for the sake of simplicity. Finally, it is important to note that the rate equations does not contain the photobleaching.

3.3 Rate Equations

The simplified version of reaction scheme is converted to the rate equations that we can simulate using computational methods. There are six differential equations which

represent the change in the population of states as follows:

$$\frac{d\rho_{gg}}{dt} = -[R_{pump}(t) + R_{probe}(t)]\rho_{gg} + \gamma_{spon}\rho_{ff} + \gamma\rho_{ss} \tag{3.1}$$

$$\frac{d\rho_{ff}}{dt} = [R_{pump}(t) + R_{probe}(t)]\rho_{gg} - [\gamma_{spon} + \gamma_{relax}]\rho_{ff} \tag{3.2}$$

$$\frac{d\rho_{ss}}{dt} = -\gamma\rho_{ss} + \gamma_{relax}\rho_{ff} + iJ(\rho_{st} - \rho_{ts}) \tag{3.3}$$

$$\frac{d\rho_{tt}}{dt} = -iJ(\rho_{st} - \rho_{ts}) \tag{3.4}$$

$$\frac{d\rho_{st}}{dt} = -\frac{\gamma}{2}\rho_{st} + i\frac{J}{2}(\rho_{ss} - \rho_{tt}) \tag{3.5}$$

$$\frac{d\rho_{ts}}{dt} = -\frac{\gamma}{2}\rho_{ts} - i\frac{J}{2}(\rho_{ss} - \rho_{tt}) \tag{3.6}$$

The rate constants in these equations are chosen as determined in the transient absorption experiments. γ_{relax} represents the singlet-born radical pair generation which is 10^{11} s^{-1}. The spontaneous emission of fluorescence occurs quickly $\gamma_{spon} = 10^9$ s^{-1}. The reverse electron transfer leads to decay from the singlet state happens with a rate constant of $\gamma = 10^6$ s^{-1}. Last but not least, the rate constant J is chosen as 10^8 s^{-1}.

3.4 Simulation Results

The main goal of our simulation is to observe effect of pump laser in the population of states and choose the probe according to the simulation results. In this method, we assumed that all molecules are in the ground state initially, and a 5 ns pump laser is applied at t = 2 μs to the sample. Immediately, the ground state population decreases as shown in Figure 3.2.

According to the simulation results, the ground state population increases after a rapid decrease due to the pump laser for the given parameters. The existence of quantum coherence alters the number of atoms turning back to the ground state.

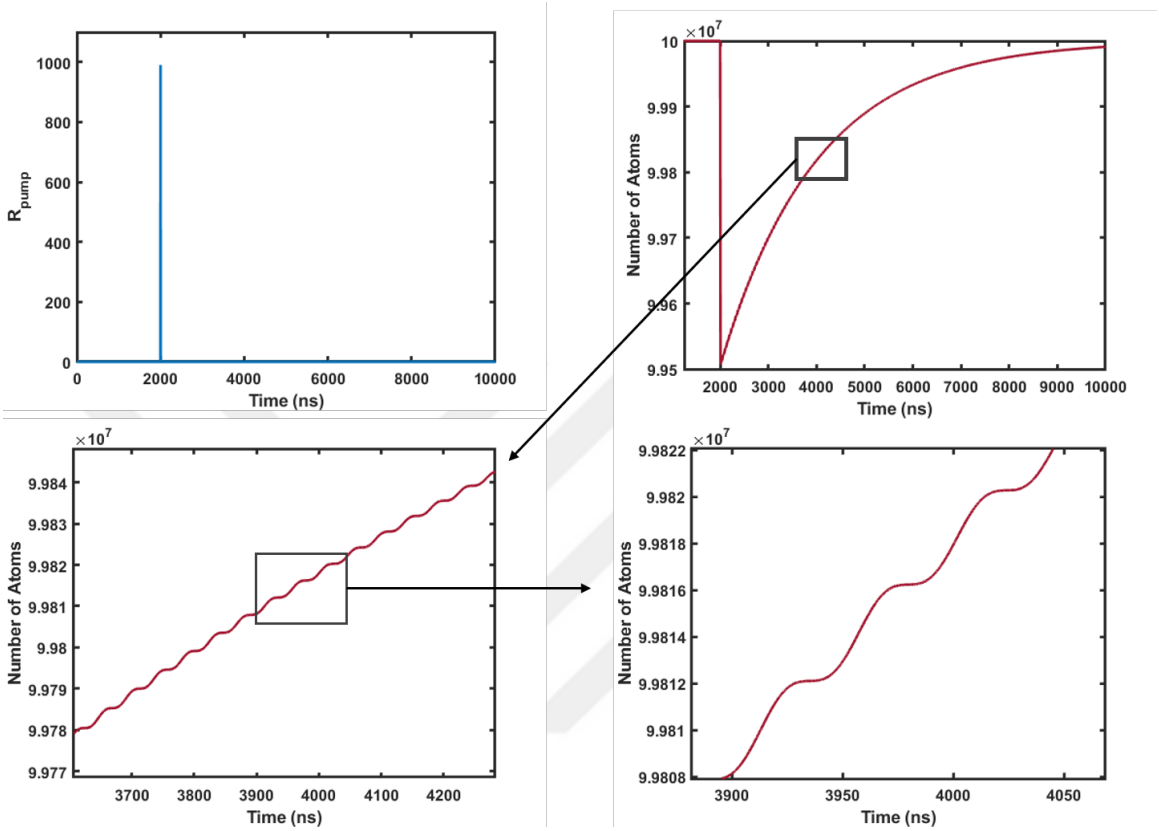

Figure 3.2: Pump laser applied in t = 2 μs to excite molecules in the ground state (upperleft). The instant reduction in the ground state with respect to the applied illimunation (upperright). The oscillation in the number of atoms which decays to the ground state from the singlet state (bottomleft). The period of oscillations is around 50 ns (bottomright).

Ideally, we can observe the ground state population with a weak probe light and detect coherent transitions. However, there are several noise components and technical limitations that should be overcomed.

The length of probe light must be smaller 50 ns because the period of oscillations is approximately 50 ns. The delay time is also important to obtain oscillations in the fluorescence data. However, since probe light is weak and short, the shot noise dominates the fluorescence data. Therefore, it is crucial to repeat the experiment in order to avoid the effect of shot noise. The number of experiment required can be adjusted by changing the concentration of sample.

Moreover, we can probe the population of the singlet state to observe coherent transitions as shown in Figure 3.3.

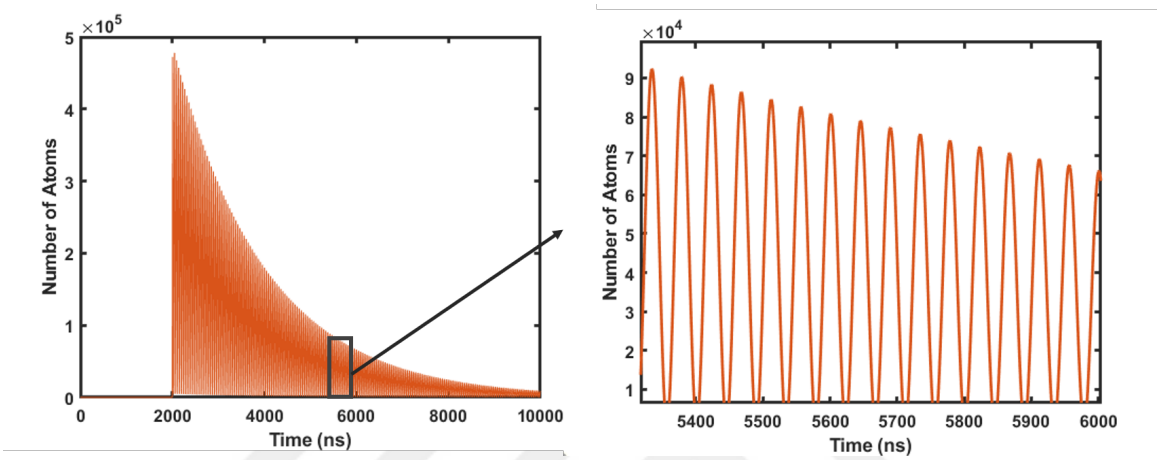

Figure 3.3: Singlet state population after the pump laser applied in t = 2 μs

However, since the singlet and triplet states are degenerate, neither absorbance nor fluorescence of the singlet state can be extracted seperately. Therefore, the only signal which indicates the transitions becomes the ground state population.

3.5 Conclusion

The magnetic field sensitivity relies on the coherent interconversion between singlet and triplet states of the radical pairs. The transition can be simulated to design an experiment which allows the detection of quantum coherence and the measurement of coherence time. However, in a basic reaction like ours, most of the reaction steps are represented with a rate constant, and their effect cannot be included. Moreover, several unavoidable effects emerging during the experiments such as shot noise or photobleaching are not introduced to our simulation; thus, we cannot estimate whether we can suppress these effects or not.

As a further improvement, we can add noise components into the simulations such as a decay for photobleaching or a poisson noise representing the shot noise. Moreover, the experimental setup which satisfies these conditions requires advanced

techniques and equipments for a synchronized sensitive measurement of fluorescence emitted.

Chapter 4

FLUORESCENCE BASED DETECTION OF MAGNETIC FIELD EFFECT ON FLAVIN CONTAINING SOLUTIONS

4.1 Background

Observation of magnetic field effect in radical pairs can be performed by probing either absorption or emission of the specific form of the molecule. As discussed in Section 1.2, absorption spectroscopy requires relatively high molecule concentration and high laser power. In addition to the consumption of sample, photodegradation is a drawback of absorption spectroscopy which is caused by high intensity laser source [56, 50]. Therefore, fluorescence microscopy comes to the fore as an alternative technique [57].

For flavoproteins or FAD containing solutions, fluorescence represents indirectly the population of ground state in case of continuous illumination. Although the ground state is not affected by the magnetic field, the number of molecules in the ground state is influenced because the reactions is spin selective. When the Zeeman effect modifies the rate of interconversion between singlet and triplet states in the presence of external magnetic field, the population of intermediate states, and the ground state change respectively. Therefore, the modulation in the fluorescence caused by the modulation in the magnetic field.

This chapter includes the experiments on the radical pair mechanism of flavin containing solutions. Although they have different reaction schemes, they both react to the presence of an external magnetic field. Several parameters affect the magnitude of this effect, which we discuss in the following sections thoroughly. However, the experimental setup should be depicted before the results of the experiments.

4.2 Experimental Setup

The aim of our experiments is to excite the flavin containing sample, and observe fluorescence emission. Our experimental setup can be divided into four units: illumination, detection, magnetic field generation and data processing. These units except data processing work coordinately for each run of the experiment, then data analyse was performed separately after requiring data.

The illumination unit contains the light source,the excitation filter and the shutter. For the light source, we employed two different lasers interchangeably. One of them is a pulsed laser at 473 nm (Coherent Chameleon 80 MHZ Ti:Sapphire pulsed laser) whereas the other one is a 450 nm continuous wave Indium Gallium Nitride laser. Since our main samples are FAD containing solution or photolyases, we selected the wavelength of the lasers in the absorption spectrum of FAD molecule to excite the sample efficiently. Other wavelength components of the laser source are precluded by the emission filter if there are any. Finally, the illumination is controlled by the shutter which is connected to the camera for synchronized data acquisition.

The inverted microscope holds the air immersion microscope objective (Nikon CFI Achro 60x 0.8 NA). The objective focuses light on the sample which is hold between two coverglasses. Fluorescence which is maximum around 520 nm is collected by the same objective and transferred to the emCCD camera (Hamamatsu) by a dichroic mirror. The sensitivity of the camera is adjustable, which is optimized for the specific experiment along with the other parameters. In addition to the fluorescence, the reflection of the light exists in the detection path; therefore, we eliminate it with low pass and bandpass filters as shown in Figure 4.1.

During the collection of fluorescence by the emCCD camera, we drive MagnaPulsa to generate square wave magnetic field whose period and duty cycle are adjustable by the user. The specifications of MagnaPulsa can be found in Appendix.

After the completion of experiments, we post-processed the data by Matlab in order to observe total fluorescence coming from the sample, and calculate the magnetic field effect (mfe). Normalized magnetic field effect in this thesis quantizes the change

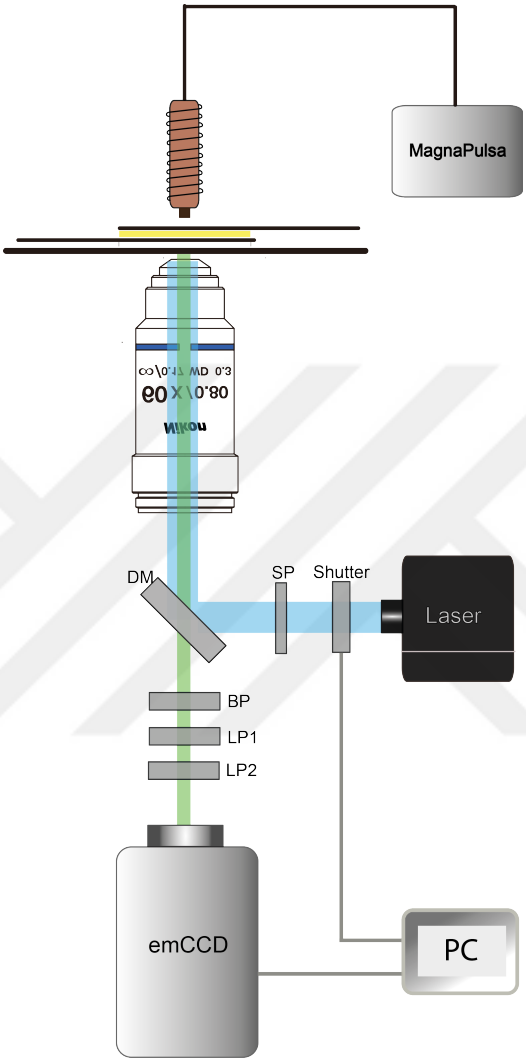

Figure 4.1: Experimental setup

in the fluorescence by the applied magnetic field. If fluorescence is a function of magnetic field strength, mfe can be written as:

$$mfe = \frac{F(B) - F(0)}{F(0)} \tag{4.1}$$

The main concern in the magnetic field calculation is photobleaching which creates a decay in the fluorescence data. The algorithms to calculate mfe are also discussed in Appendix.

4.3 Reaction Scheme

Flavin can be found in two molecule forms: FAD (flavin adenine dinucleotide) and FMN (flavin mononucleotide) which are simpler and more stable than flavoproteins. Therefore, they have advantageous over the proteins in order to understand radical pair mechanism. However, they differ from flavoproteins in reaction scheme.

Flavin in the form of FMN or fully oxidized FAD can absorb blue light ($F \rightarrow {}^1F^*$). Excited flavin can either emit fluorescence or undergo ISC (${}^1F^* \rightarrow {}^3F^*$). Intermolecular electron transfer between the triplet flavin and a donor generates the triplet radical pair (${}^3[F^{\bullet -} + D^{\bullet +}]$). As shown in Figure 4.2, triplet radical pairs inter-converts singlet radical pairs coherently in the absence of an external magnetic field.

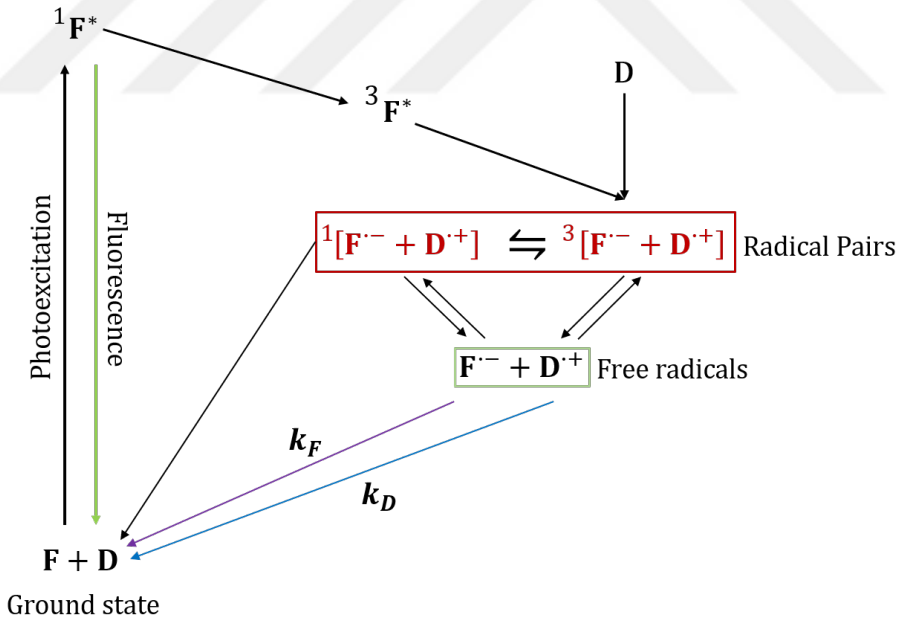

Figure 4.2: Reaction scheme of the FAD containing solutions [6]

Radical pairs can split in to two radicals if they diffuse apart from each other and also merge to form pairs in either triplet or singlet form. The singlet radical pair can return to ground state by a reverse electron transfer.

In the presence of an external magnetic field, two of the triplet states isolate and the interconversion rate reduces. The population of singlet state and the ground

state decreases with respect to the magnetic field. The reduction in the ground state population directly impacts the fluorescence which we can observe by our experimental setup.

4.4 Results

The aim of the experiment in this chapter is to investigate radical pair mechanism easily, since FAD and tryptophan molecules are not sensitive to the environmental conditions as proteins and they can exhibit response to an applied magnetic field.

As shown in Figure 4.3, 1 μM FAD and 300 μM Trp solution in a citric acid buffer (pH = 2.3) reacts to 28 mT square wave magnetic field with a period of 700 ms and duty cycle of 28.57%. The magnetic field effect is calculated as -2.25% for

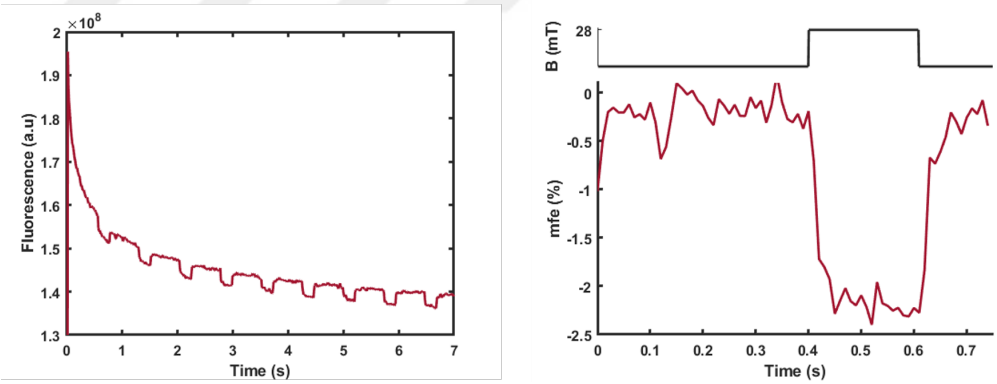

Figure 4.3: Effect of 28 mT square wave magnetic field to the fluorescence of 1 μM FAD and 300 μM Trp (left) and mfe for one period of magnetic field (right)

2.14 mW laser power (450 nm) at the back aperture of the microscope objective. The magnetic field effect is in agreement with the reaction scheme shown in Figure 4.2. In the presence of 28 mT magnetic field, the singlet state population and ground state population decrease.

Although the magnetic field effect is observable from the fluorescence data in time domain, the Fourier transform of the fluorescence data is generated to compare with the Fourier transform of the magnetic field strength as illustrated in Figure 4.4.

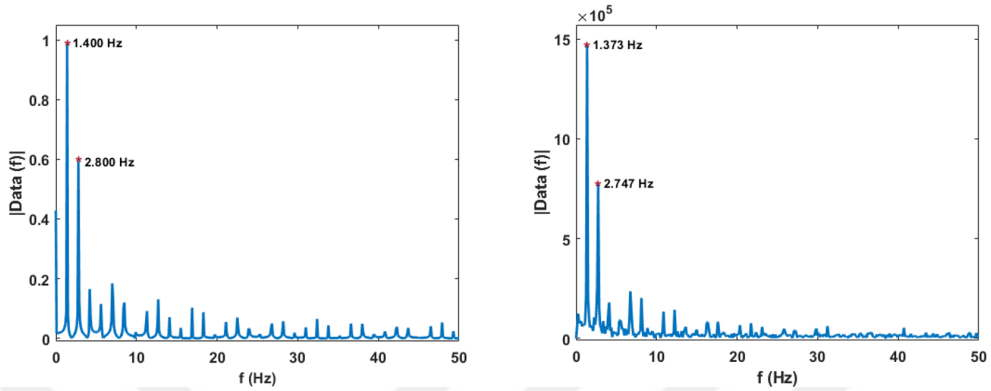

Figure 4.4: FFT of the fluorescence emitted by 1 μM FAD and and 300 μM Trp in the presence of 28 mT square wave magnetic field (left), FFT of the magnetic field signal (right)

Fourier transform shows that the radical pair mechanism reacts to the magnetic field effect immediately. We also check the effect of longer magnetic field exposure to the solution. For this experiment, a permenant magnet is utilized, and it is moved towards the sample manually. We repeated it twice for a longer data acquisition time intervals. As you can see in Figure 4.5, the applied magnetic field decreases the fluorescence as long as the magnetic field is applied.

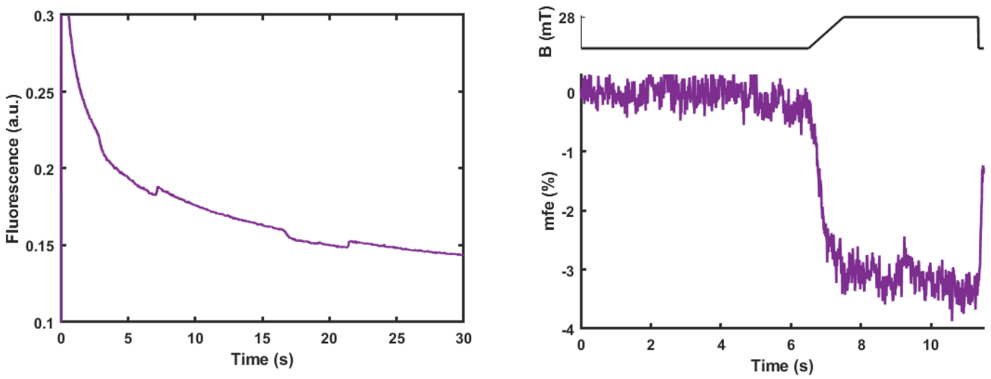

Figure 4.5: Effect of 28 mT magnetic field produced by a permanent magnet for 1 μM FAD and 300 μM Trp

In the continuous illumination, there is continuous flow to the triplet channel for triplet born radical pair. The applied external magnetic field maintains energy level

separation which prevents transition to singlet state from the triplet states. Furthermore, it is important to understand the reason of the decay in the fluorescence level with respect to time. Therefore, we check the emission spectrum of FAD. According to Figure 4.6, the fluorescence level is decreasing even without any magnetic field, and the maximum wavelength is unchanged. We also solve fluorescein dye absorbing in

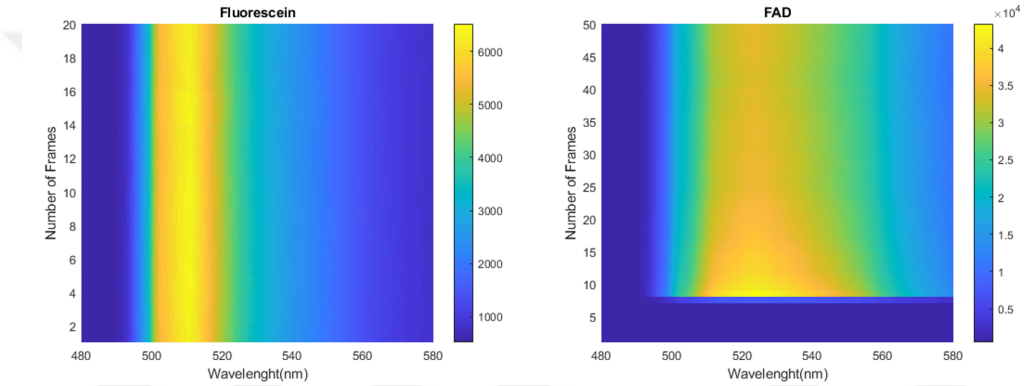

Figure 4.6: Emission spectroscopy of FAD molecules (left) and fluorescein (right) in an acidic solution, excited by 473 nm pulsed laser

the same acidic buffer as FAD, and measure the emission spectrum at the same wavelength as shown in Figure 4.7. Unlike FAD, fluorescein emits fluorescence without a decay. Therefore, the fluorescence decays because of photobleaching.

The next task is to discover the acceptor and the donor in a flavin containing solution. 450 nm laser excites the flavin, and flavin part can be found in both FAD and FMN. However, two major candidates for donor molecules are Adenine and Tryptophan.

Solution	Magnetic Field Effect
FAD	Yes
FAD + Tryptophan	Yes
FMN	No
FMN + Tryptophan	Yes

Table 4.1: Magnetic fied effect on flavin containing solutions

According to the results, FAD can transfer electron from both Adenine and Tryptophan to form radical pair. FMN and Tryptophan pairs are also sensitive to the magnetic field. However, the solutions that contains only FMN does not react to the magnetic field. Therefore, it is obvious that the magnetic sensitivity relies on the generation of radical pairs by an electron transfer.

Another parameter for the radical pair mechanism is pH of the solution buffer which can modify the molecular structure, enhance or inhibit the electron transfer. It is crucial to determine its effect on the reaction scheme. For a FAD containing solution, we only change the pH value. Therefore, we expected to measure the fluorescence at the same level which is not the result as shown in Figure 4.7.

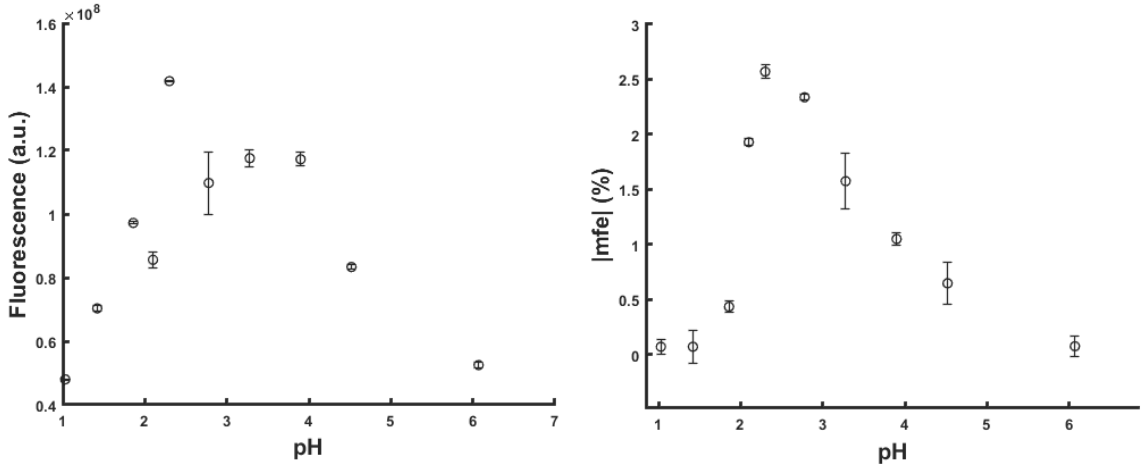

Figure 4.7: pH dependence of fluorescence and magnetic field effect for 1 μM FAD and 300 μM Trp solution

As discussed in [58], pH has a significant impact on the conformational change, which can alter the absorption and emission wavelengths. Moreover, we observe the degradation of solutions whose pH are larger than 4.06. There is a possible chance to end up with solutions with lower concentration of FAD than the initially prepared. Further investigation of pH is highly required to differentiate which mechanism inhibits the fluorescence and mfe for higher and lower pH values.

Laser intensity dependence of the magnetic field effect must be also characterized to optimize the experiments. We aim to obtain highest possible signal to measure magnetic field effect. Besides, we prefer to avoid photobleaching by reducing the laser intensity. There is a trade of between signal level and photobleacing. As you can see in Figure 4.8, around 7 mW laser power on the back aperture of the microscope objective, the fluorescence level is saturated by photobleaching.

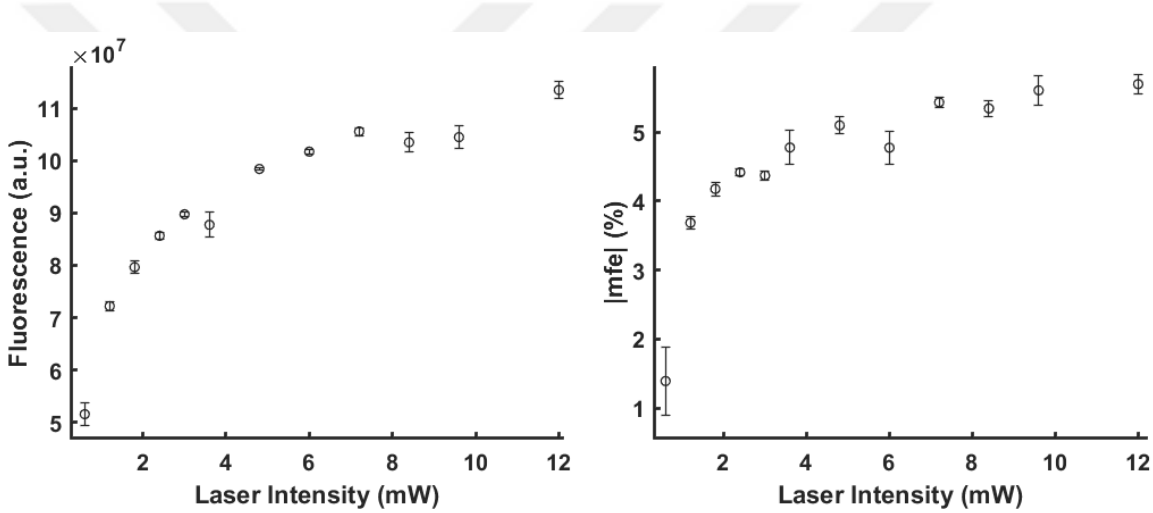

Figure 4.8: Fluoresence (left) and mfe (right) with respect to the laser power at the back aperture of the microscope objective

Although we can explain the saturation in the fluorescence level with respect to the laser intensity, it is interesting to observe saturation in the mfe. Assume that the ground state population is similar, mfe must be larger for higher intensities because the rate is higher which is not clear in our data.

Last but not least, we check the energy level splitting by changing the magnetic field strength. As we can see in Figure 4.9, mfe increases with increasing magnetic field.

The saturation around 15-20 mT is also expected. Once the energy difference between triplet states increase, the interconversion rate decreases. However, since the excitation power is the same, the number of molecule in singlet state will be the same

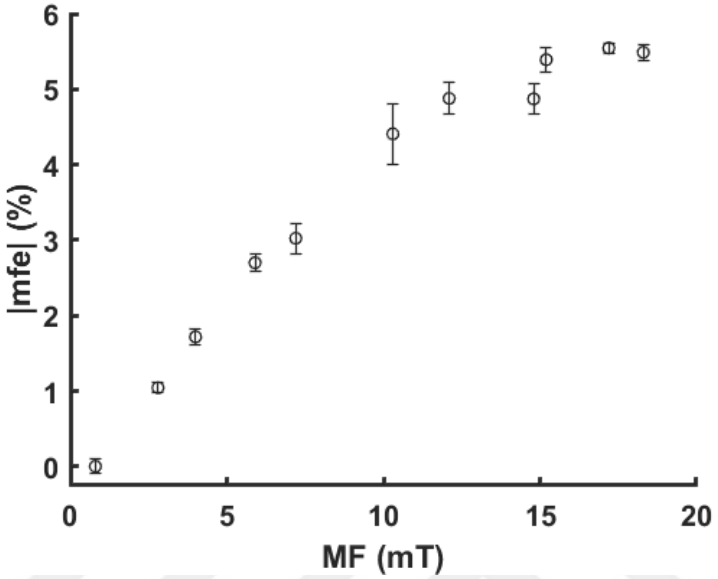

Figure 4.9: Magnetic field effect with respect to the magnetic field strength on the sample

after triplet states have enough energy differences for isolation.

4.5 Conclusion

Our fluorescence based experiments on flavin containing solutions achieve to detect the effect of 28 mT magnetic field up to 5.5% depending on the parameters such as laser intensity. Moreover, although the lifetimes of the states are not observed due to the continuous illumination, our methods successes to investigate he effect of several parameters on the magnetic field sensitivity.

As a future direction, the saturation in the magnetic field effect with respect to the laser intensity (Figure 4.8) should be investigated using flavin containing solutions. Although flavin contaning solutions and photolyases have different reaction schemes, these experiments explain many steps in the reaction schemes.

Chapter 5

FLUORESCENCE-BASED DETECTION OF MAGNETIC FIELD EFFECT ON PHOTOLYASES

5.1 Background

Detection of magnetic field effect on cryptochromes and photolyases is more challenging than the flavin containing solutions because proteins are more complex and more sensitive to the environmental conditions such as temperature, pH or light. Therefore, they require a controllable experimental setup. However, we aim to utilize the same experimental setup (Figure 4.1). There have been studies which analyses the mfe on crytochromes and photolyases by transient absorption spectroscopy [51, 52, 59]; however, fluorescence based techniques has been recently applied to experiments with proteins [6].

In this chapter, our purpose is to investigate the radical pair mechanism for cryptochromes and photolyases which are the candidate molecules for avian compass system. We also propose future directions to understand the reaction scheme of flavoproteins.

5.2 Reaction Scheme

Crytochromes and photolyases are two flavoproteins which can play a role in magnetic compass system. They contain FAD and Trp-triad (Trp_A, Trp_B, Trp_C) as an electron transfer chain. The distance between FAD and the nearest Trp (Trp_A) or so called terminal residue is 7.4 Å, allows rapid electron transfer. However, cryptochromes and photolyases differ from flavin containing solutions in reaction scheme.

Flavin in the form of fully oxidized FAD can absorb blue light ($F \rightarrow {}^1F^*$). Excited

flavin can either emit fluorescence or take electron from Trp_A which occurs rapidly to form radical pair in the singlet state as shown in Figure 5.1. The transfer of electron from Trp_A to FAD is followed by the sequential electron transfer from Trp_B to Trp_A, and Trp_C to Trp_B.

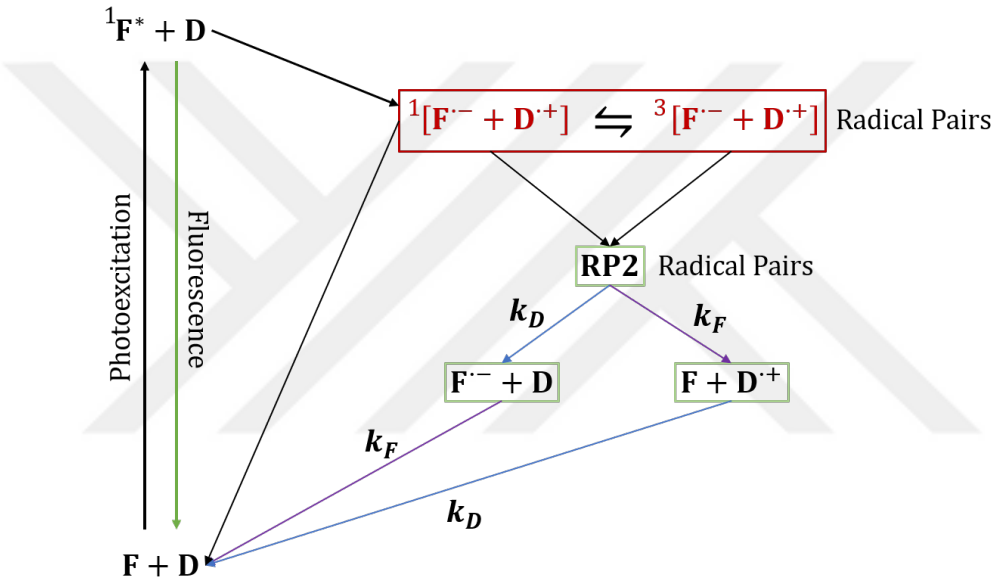

Figure 5.1: Reaction scheme of crypthochromes and photolyases [6]

For the solutions, radical pairs can split in to two radicals if they diffuse apart from each other and also they can merge to form pairs in either triplet or singlet form. However, in cryptochrome, they have a fixed position. Therefore, second radical pair (RP2) can be formed by protanation of flavin radical or deprotonation of the donor or both [6] which do not react to the magnetif field. Moreover, the singlet radical pair can return to ground state by a reverse electron transfer.

In the presence of an external magnetic field, two of the triplet states isolate and the interconversion rate reduces. The population of singlet state and the ground state increases with respect to the magnetic field because the radical pair is singlet born. The increase in the ground state population directly impacts the fluorescence which we can observe by our experimental setup.

5.3 Results

According to our experiments, 170 μM VcPHR (*Vibrio cholerae* photolyase) in Tris buffer (20 mM Tris-HCl, 200 mM NaCl, 1 mM EDTA and 50% glycerol, pH = 7.4) reacts to the 28 mT magnetic field as shown in Figure 5.2.

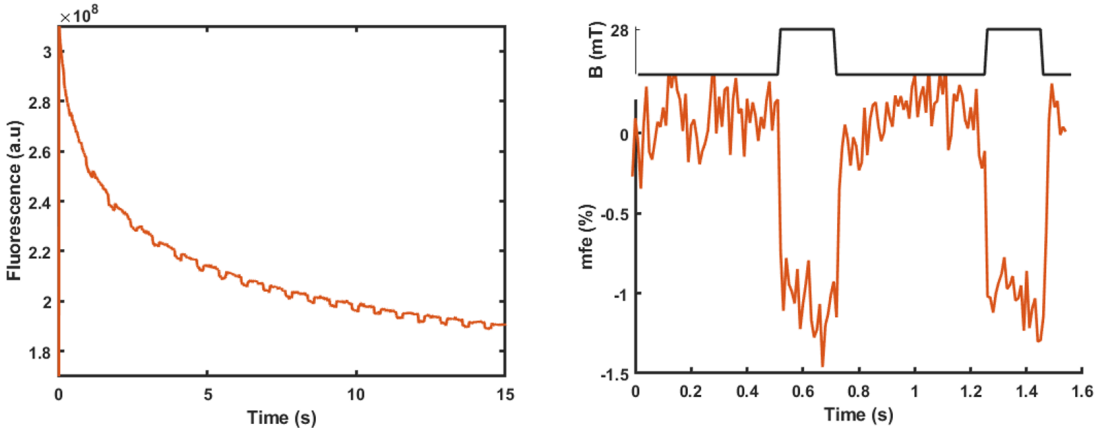

Figure 5.2: Effect of 28 mT square wave magnetic field to the fluorescence of 170 μM VcPHR (left) and mfe for one period of magnetic field (right)

The average magnetic field effect for this experiments is -1.32%. Moreover, we conduct experiments on 166 μM EcPHR (*Escherichia coli* photolyase) solution as you can see in Figure 5.3. The magnetic field effect is -1.01% for this protein in the HEPES buffer (25mM Hepes, 100 mM NaCl, 1 mM EDTA, 1 mM NaN_3, 50% glycerol and pH = 7.4).

These two experiments show a reduction in the fluorescence data in the presence of an external magnetic field, although an increase is expected because of the singlet born radical pair mechanism given in Figure 5.1. Moreover, the transient absorption experiments in the literature [51, 59, 60] observed a positive magnetic field on EcPHR and AtCRY proteins, and [6] detected the positive mfe on AtCRY by using fluorescence based measurements. Therefore, the differences in protein sample preparation become crucial for our case and previously suggested methods in the literature.

In addition to the FAD, photolyases can contain another lower wavelength light

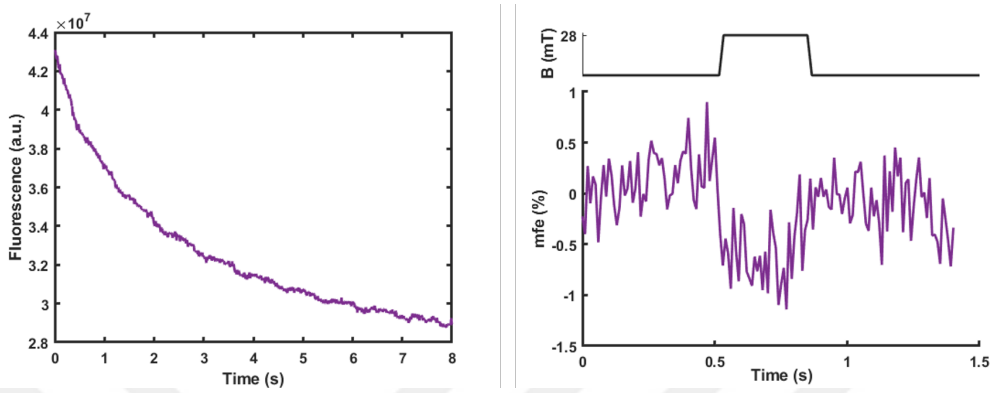

Figure 5.3: Effect of 28 mT square wave magnetic field to the fluorescence of 166 μM EcPHR (left) and mfe for one period of magnetic field (right)

receptor molecule called MTHF (methylene tetrahydrofolate) [61]. This molecule plays an important role in DNA repair by absorbing UV light. In this mechanism, the photoexcitation of MTFH is followed by FRET mechanism between MTHF and FAD that have distance of 16.8 Å [61]. Considering the complexity of proteins, this mechanism can affect the radical pair mechanism for only our case because some of the previous works intentionally remove MTHF to avoid unwanted signals [59, 51].

Another condition that must be satisfied before the photoexcitation of FAD is to make sure that all FADs are in fully oxidized form. Pretreatments with potassium ferricyanide can be performed to oxidize all FAD molecules beforehand [51].

As a future work, we aim to check the effect of these modification for our proteins. Moreover, we can try to excite these proteins in the wavelegnth of MTHF absorption and check the FRET mechanism.

On the other hand, our experiments are self-consistent as you can see in Figure 5.4. The Fourier transform of the modulation is also matched with the Fourier transform of magnetic field applied with MagnaPulsa.

We also apply 12 mT magnetic field to the VcPHR solution during 5 s. The duration of the magnetic field does not have any impact, the fluorescence level decreases with respect to the magnetic field strength.

We also changed the magnetic field strength for the experiments with permanent

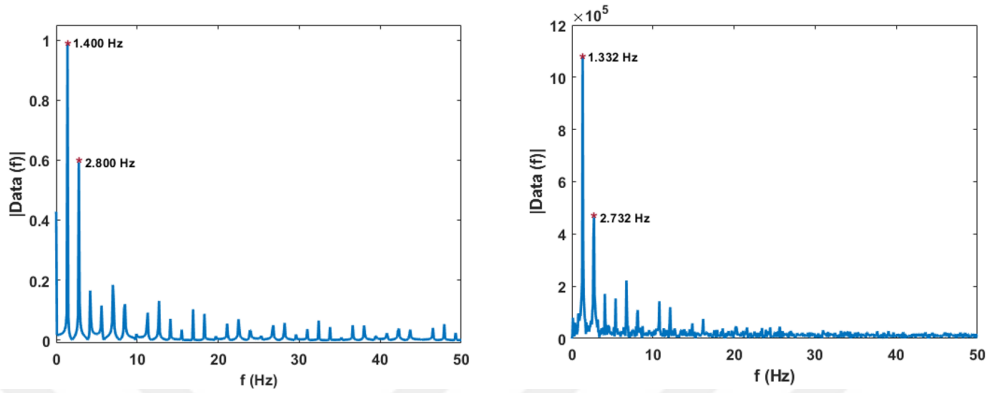

Figure 5.4: FFT of the fluorescence emitted by 170 μM VcPHR sample in the presence of 28 mT square wave magnetic field (left), FFT of the magnetic field signal (right)

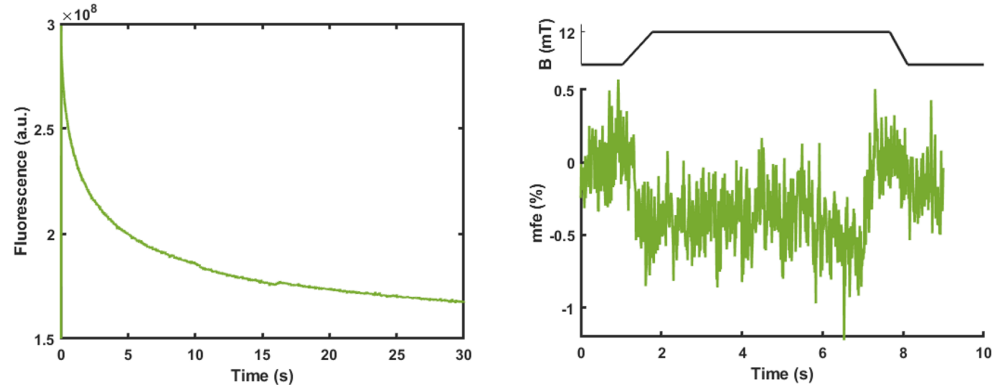

Figure 5.5: Effect of 12 mT square wave magnetic field on the fluorescence of 170 μM VcPHR (left). mfe shown for one period (right)

magnet and obtained the values in Table 5.1 for 170 μM VcPHR.

Magnetic Field Strength (mT)	mfe (%)
6	-0.21
12	-0.30
21	-0.60
70	-1.29

Table 5.1: Magnetic field effect on 170 μM VcPHR, magnetic fields are applied by the permenant magnet

In addition to the modulation in the fluorescence, there is also a decay which

represents the presence of photobleaching in both Figure 5.2 and Figure 5.4.

5.4 Conclusion

The magnetic field effect on flavoproteins is also detected using our fluorescence based technique. The differences in the protein structures results in the negative magnetic field effect on proteins. Therefore, we aim to explain the reason behind triplet born radical pair mechanism in this experiment.

In addition to the research on the reaction mechanism, we are motivated to observe orientation dependence of the magnetic field effect. Since the crytochromes are important to study in this manner, we aim to enhance our techniques to reach single molecule fluorescence observations.

Chapter 6

FRET ENHANCEMENT TO FLUORESCENCE MICROSCOPY

6.1 Background

Flavoproteins are complex molecules, and they are challenging to investigate. In recent years, the artificial structures have been generated to understand several parameters which play important role in the magnetic field effect [62, 63]. One method to create an artificial molecules is Förster Resonance Energy Transfer (FRET) by dye conjugation. FRET is an energy transfer from donor to acceptor without any photon emission from the donor [64]. Besides, it is well-known and widely used in the observation of biological samples by fluorescence microscopy.

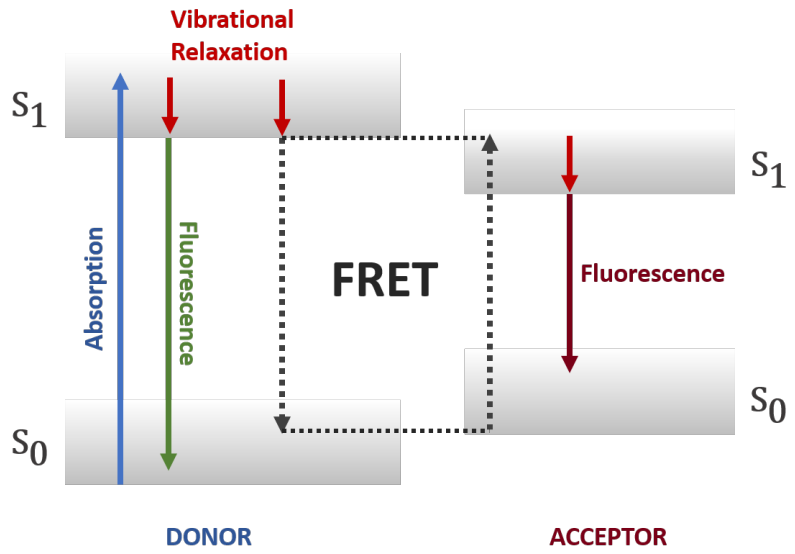

Figure 6.1: Jablonski diagram of FRET mechanism. S_0 and S_1 represent the ground state and first excited state respectively.

As illustrated in Figure 6.1, the energy levels of two molecules must overlap. In other words, the emission spectrum of the donor must overlap with the absorption spectrum of the acceptor [64]. Moreover, the distance between donor and acceptor impacts the FRET rate dramatically.The rate is calculated as [64]:

$$k_T(r) = -\frac{1}{\tau_D}\left(\frac{R_0}{r}\right)^6 \tag{6.1}$$

τ_D is the lifetime of donor molecule without any FRET mechanism. R_0 is the Förster distance and, it is typically 2-9 nm which is suitable for the dye attachment to flavoproteins and FAD.

In addition to the distance requirement, FRET acceptor must satisfy spectral overlap with the emission spectrum of flavin, and it must not be affected by the external magnetic field.

Above mentioned issues as well as the possibility of FRET mechanism are discussed in this chapter for photolyases and flavin containing solutions separately.

6.2 FRET for Photolyases

Dye conjugation to proteins has been a well understood process amongst biologists, and there are various methods to attach dye molecule to the surface of proteins. One of them is NHS ester conjugation [65]. As described in Figure 6.2, a dye molecule (NHS Ester Reagent) can connect to any amine group in the protein surface [66]. this type of conjugation can produce stable attachment for our experiments.

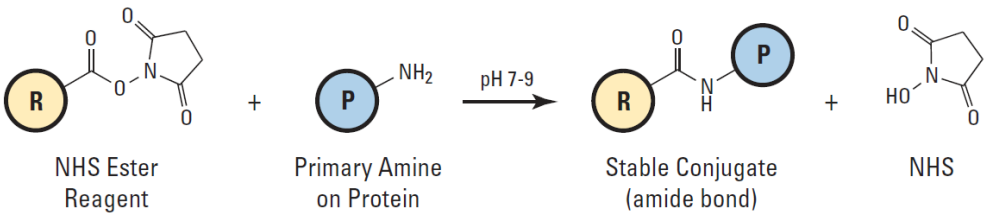

Figure 6.2: NHS Ester conjugation for protein-dye attachment. R denotes the dye molecule, and P represents proteins [66]

Photolyases posses aminoacids like the other proteins. Amongst these aminoacids, lysine has amine group, and it can accept dye molecules if it is located on the protein surface. cryptochromes and photolyases have more than 10 lysines on their surfaces as illustrated with red in Figure 6.3.

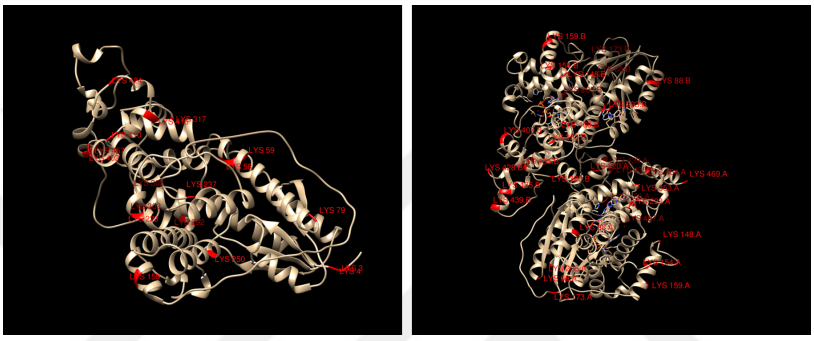

Figure 6.3: Lysine aminoacids(red) in the flavoproteins: VcCRY1 (left) and EcPHR (right)

In the selection of a proper dye, three requirements must be satisfied: 1) Suitability for NHS ester bound, 2) spectral overlap, and 3) no magnetic sensitivity. Several dyes for the NHS ester conjugation are available in the market; for instance, ATTO 565 NHS Ester or ATTO 590 NHS Ester can overap with the energy levels of singlet and triplet states.

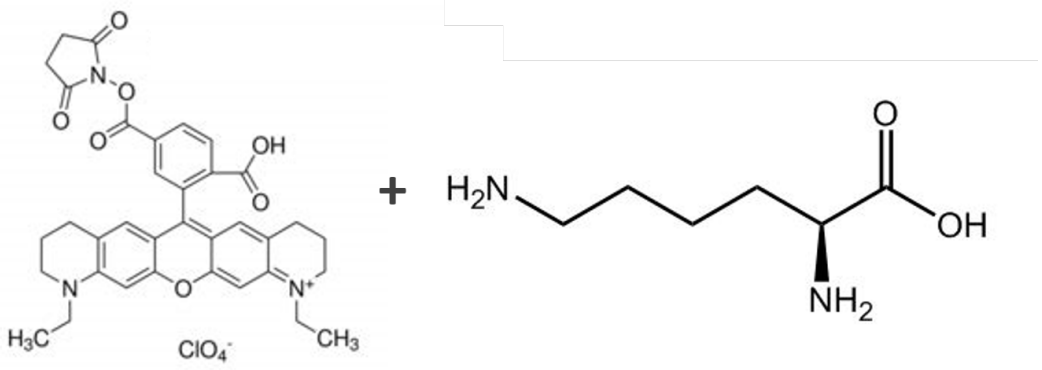

Figure 6.4: Molecular structures of ATTO 565 NHS Ester (left) and Lysine (right) which are the two components of the dye conjugation for FRET mechanism

However, it is crucial to note that NHS Ester conjugations must be performed in

a amin-free buffer such as HEPES. Otherwise, dyes sticks to the buffer, instead of lysine aminoacids.

The magnetic field experiments with ATTO dyes do not demonstrate any magnetic sensitivity. Therefore, they can be conjugated to proteins to modify the reaction scheme.

The FRET mechanism between a photolyase and an acceptor dye updates the reaction scheme as follows:

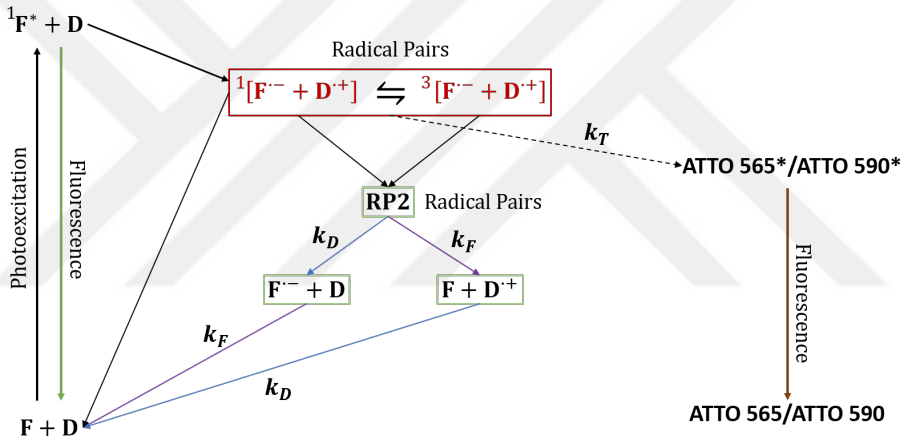

Figure 6.5: Reaction scheme of radical pair mechanism with FRET modification for singlet born radical pairs

Due to the degeneracy of singlet and triplet states, the acceptor is able to couple to all four states in the absence of any external magnetic field. However, according to the k_T value, FRET mechanism can dominate the reaction scheme, and it might suppress the generation of the second radical pair.

6.3 FRET for Flavin Containing Solutions

FAD and dye attachments is relatively more complicated than the dye conjugation to proteins. In our case, we aim to attach 5(6)-Carboxy-X-rhodamine to alloxazine, the core of flavin molecule.

The attachment of the dye molecule to the flavin core, will allow FRET mechanism

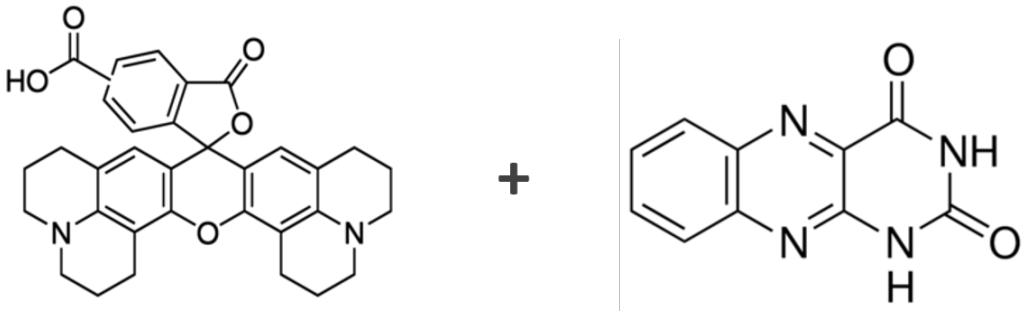

Figure 6.6: Molecular structures of 5(6)-Carboxy-X-rhodamine (left) and alloxazine (right) which are the two components of the dye attachments for FRET mechanism

since the distance betwen them will be very small. Hence, the reaction scheme is updated as follows:

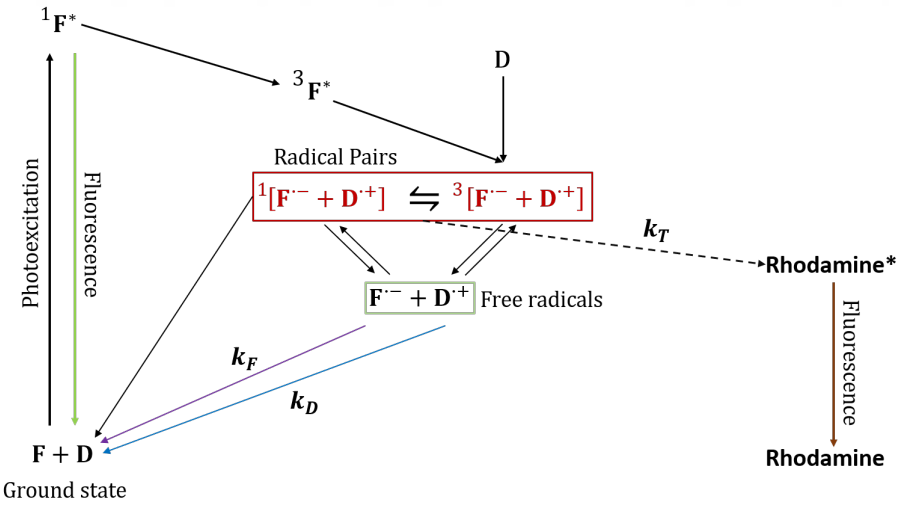

Figure 6.7: Reaction scheme of radical pair mechanism with FRET modification for triplet born radical pairs

Due to the degeneracy of singlet and triplet states, the acceptor is able to couple with all four states in the absence of any external magnetic field like the singlet born radical pairs. However, according to the k_T value, FRET mechanism can dominate the reaction scheme, and it can enhance the decay to the ground state.

6.4 Conclusion and Further Work

The issues in this chapter is still under investigation and it is a future direction for us. The dye attachment to the protein and flavin is quite challenging. However, FRET mechanism will open a new discussion by modifying the reaction scheme.

In addition to the application of flavin as a donor, we can find a donor such as MTHF in crytochromes to built FRET mechanism. This also change the reaction scheme since it eliminates the photoexcitation of FAD. This can be interesting in terms of photobleaching as well.

Chapter 7

CONCLUSION AND OUTLOOK

The radical pair based model has been studied over the years, and it is still a challenging purpose to pursue. Discovering its relation with the avian compass system will not only solve the mechanism of magnetoreception but it will also lead to the research area which focuses on the effect of low magnetic fields on biological processes. Therefore, we aim to observe the magnetic sensitivity of radical pairs and enhance the observation techniques.

The experiments demonstrated in this thesis require the theoretical knowledge of spin chemistry and quantum interactions. Moreover, the electron transfer mechanism must be studied thoroughly. The electron transfer mechanism and lifetime of states are also significant concepts to address (Chapter 2).

The magnetically sensitive part of the mechanism relies on the coherent transitions between singlet and triplet states. Although it can be observed indirectly; for instance, by applying magnetic field, we discussed the possibility of the fluorescence based experiments to observe these transitions in Chapter 4. As an outlook, we aim to add environmental conditions to the simulations.

Observation of magnetic field effect on flavin containing solutions and photolyases is achieved. We also investigated the effect of pH, laser intensity and magnetic field strength easily thank to fluorescence based techniques (Chapter 4). We also conducted experiments on VcPHR and EcPHR which are more complicated than FAD molecule. The results of these experiments create a path for us to further understand the reaction scheme for proteins (Chapter 5).

We also introduced one of our short term goals: FRET mechanism between flavin and a dye. This artificial structure is aimed to modify the reaction scheme, and it can

lead to enhanced fluorescence level. As an outlook, we aim to achieve higher fluorescence signal to go single-molecule level detection of magnetic field effect. Formation of FRET mechanism presented in this thesis will serve to this mission.

BIBLIOGRAPHY

[1] D. Budker and M. Romalis, "Optical magnetometry," *Nature Physics*, vol. 3, no. 4, p. 227, 2007.

[2] K. Wüthrich, "Nmr with proteins and nucleic acids," *Europhysics News*, vol. 17, no. 1, pp. 11–13, 1986.

[3] C. A. Dodson, P. J. Hore, and M. I. Wallace, "A radical sense of direction: signalling and mechanism in cryptochrome magnetoreception," *Trends in Biochemical Sciences*, vol. 38, no. 9, pp. 435–446, 2013.

[4] P. J. Hore, "Upper bound on the biological effects of 50/60 hz magnetic fields mediated by radical pairs," *eLife*, vol. 8, p. e44179, 2019.

[5] P. L. Bounds and N. Kuster, "Is cryptochrome a primary sensor of extremely low frequency magnetic fields in childhood leukemia?," *Biophysical Journal*, vol. 108, no. 2, p. 562a, 2015.

[6] D. R. Kattnig, E. W. Evans, V. Déjean, C. A. Dodson, M. I. Wallace, S. R. Mackenzie, C. R. Timmel, and P. Hore, "Chemical amplification of magnetic field effects relevant to avian magnetoreception," *Nature Chemistry*, vol. 8, no. 4, p. 384, 2016.

[7] T. P. Quinn, R. T. Merrill, and E. L. Brannon, "Magnetic field detection in sockeye salmon," *Journal of Experimental Zoology*, vol. 217, no. 1, pp. 137–142, 1981.

[8] D. Shcherbakov, M. Winklhofer, N. Petersen, J. Steidle, R. Hilbig, and M. Blum,

"Magnetosensation in zebrafish," *Current Biology*, vol. 15, no. 5, pp. R161–R162, 2005.

[9] P. Light, M. Salmon, and K. J. Lohmann, "Geomagnetic orientation of loggerhead sea turtles: evidence for an inclination compass," *Journal of Experimental Biology*, vol. 182, no. 1, pp. 1–10, 1993.

[10] P. Němec, J. Altmann, S. Marhold, H. Burda, and H. H. Oelschläger, "Neuroanatomy of magnetoreception: the superior colliculus involved in magnetic orientation in a mammal," *Science*, vol. 294, no. 5541, pp. 366–368, 2001.

[11] S. Marhold, W. Wiltschko, and H. Burda, "A magnetic polarity compass for direction finding in a subterranean mammal," *Naturwissenschaften*, vol. 84, no. 9, pp. 421–423, 1997.

[12] W. Wiltschko and R. Wiltschko, "Magnetoreception in birds: two receptors for two different tasks," *Journal of Ornithology*, vol. 148, no. 1, pp. 61–76, 2007.

[13] P. Thalau, T. Ritz, H. Burda, R. E. Wegner, and R. Wiltschko, "The magnetic compass mechanisms of birds and rodents are based on different physical principles," *Journal of the Royal Society Interface*, vol. 3, no. 9, pp. 583–587, 2006.

[14] P. J. Hore and H. Mouritsen, "The Radical-Pair Mechanism of Magnetoreception," *Annual Review of Biophysics*, vol. 45, no. 1, pp. 299–344, 2016.

[15] W. Wiltschko, "ber den einflu statischer magnetfelder auf die zugorientierung der rotkehlchen (erithacus rubecula)," *Zeitschrift fur Tierpsychologie*, vol. 25, no. 5, pp. 537–558, 1968.

[16] R. Wiltschko and W. Wiltschko, "Evidence for the use of magnetic outward-journey information in homing pigeons," *Naturwissenschaften*, vol. 65, pp. 112–113, Feb 1978.

[17] W. Wiltschko and R. Wiltschko, "Migratory orientation of european robins is affected by the wavelength of light as well as by a magnetic pulse," *Journal of Comparative Physiology A*, vol. 177, pp. 363–369, Sep 1995.

[18] W. Wiltschko and R. Wiltschko, "Magnetic compass of european robins," *Science*, vol. 176, no. 4030, pp. 62–64, 1972.

[19] R. Wiltschko and W. Wiltschko, "Directional orientation of birds with the help of the magnetic field under different light conditions," *Nature Nanotechnology*, vol. 19, pp. 523–551, 2010.

[20] J. L. Kirschvink and J. L. Gould, "Biogenic magnetite as a basis for magnetic field detection in animals," *Biosystems*, vol. 13, no. 3, pp. 181–201, 1981.

[21] J. L. Kirschvink and M. M. Walker, "Particle-size considerations for magnetite-based magnetoreceptors," in *Magnetite Biomineralization and Magnetoreception in Organisms*, pp. 243–254, Springer, 1985.

[22] J. L. Kirschvink, M. M. Walker, and C. E. Diebel, "Magnetite-based magnetoreception," *Current Opinion in Neurobiology*, vol. 11, no. 4, pp. 462–467, 2001.

[23] S. Johnsen and K. J. Lohmann, "The physics and neurobiology of magnetoreception," *Nature Reviews Neuroscience*, vol. 6, no. 9, p. 703, 2005.

[24] J. L. Kirschvink, M. Winklhofer, and M. M. Walker, "Biophysics of magnetic orientation: strengthening the interface between theory and experimental design," *Journal of the Royal Society Interface*, vol. 7, no. suppl_2, pp. S179–S191, 2010.

[25] H. Mouritsen, "Neurosciences-from molecule to behavior: a university textbook (pp. 427–443)," 2013.

[26] H. Mouritsen, "Sensory biology: search for the compass needles," *Nature*, vol. 484, no. 7394, p. 320, 2012.

[27] H. Mouritsen, "Magnetoreception in birds and its use for long-distance migration," in *Sturkie's avian physiology*, pp. 113–133, Elsevier, 2015.

[28] C. V. Mora, M. Davison, J. M. Wild, and M. M. Walker, "Magnetoreception and its trigeminal mediation in the homing pigeon," *Nature*, vol. 432, no. 7016, p. 508, 2004.

[29] M. Zapka, D. Heyers, C. M. Hein, S. Engels, N.-L. Schneider, J. Hans, S. Weiler, D. Dreyer, D. Kishkinev, J. M. Wild, *et al.*, "Visual but not trigeminal mediation of magnetic compass information in a migratory bird," *Nature*, vol. 461, no. 7268, p. 1274, 2009.

[30] N. J. Turro and B. Kraeutler, "Magnetic field and magnetic isotope effects in organic photochemical reactions. a novel probe of reaction mechanisms and a method for enrichment of magnetic isotopes," *Accounts of Chemical Research*, vol. 13, no. 10, pp. 369–377, 1980.

[31] K. Schulten, C. E. Swenberg, and A. Weller, "A biomagnetic sensory mechanism based on magnetic field modulated coherent electron spin motion," *Zeitschrift für Physikalische Chemie*, vol. 111, no. 1, pp. 1–5, 1978.

[32] C. T. Rodgers, "Magnetic field effects in chemical systems," *Pure and Applied Chemistry*, vol. 81, no. 1, pp. 19–43, 2009.

[33] U. E. Steiner and T. Ulrich, "Magnetic field effects in chemical kinetics and related phenomena," *Chemical Reviews*, vol. 89, no. 1, pp. 51–147, 1989.

[34] J. Woodward, "Radical pairs in solution," *Progress in Reaction Kinetics and Mechanism*, vol. 27, no. 3, pp. 165–207, 2002.

[35] W. Wiltschko, U. Munro, H. Ford, and R. Wiltschko, "Red light disrupts magnetic orientation of migratory birds," *Nature*, vol. 364, no. 6437, p. 525, 1993.

[36] M. Kondoh, C. Shiraishi, P. Müller, M. Ahmad, K. Hitomi, E. D. Getzoff, and M. Terazima, "Light-induced conformational changes in full-length arabidopsis thaliana cryptochrome," *Journal of Molecular Biology*, vol. 413, no. 1, pp. 128–137, 2011.

[37] C. L. Partch, M. W. Clarkson, S. Özgür, A. L. Lee, and A. Sancar, "Role of structural plasticity in signal transduction by the cryptochrome blue-light photoreceptor," *Biochemistry*, vol. 44, no. 10, pp. 3795–3805, 2005.

[38] T. Ritz, S. Adem, and K. Schulten, "A model for photoreceptor-based magnetoreception in birds," *Biophysical Journal*, vol. 78, no. 2, pp. 707–718, 2000.

[39] H. Mouritsen, G. Feenders, M. Liedvogel, and W. Kropp, "Migratory birds use head scans to detect the direction of the earth's magnetic field," *Current Biology*, vol. 14, no. 21, pp. 1946–1949, 2004.

[40] M. Ahmad and A. R. Cashmore, "Hy4 gene of a. thaliana encodes a protein with characteristics of a blue-light photoreceptor," *Nature*, vol. 366, no. 6451, p. 162, 1993.

[41] A. R. Cashmore, J. A. Jarillo, Y.-J. Wu, and D. Liu, "Cryptochromes: blue light receptors for plants and animals," *Science*, vol. 284, no. 5415, pp. 760–765, 1999.

[42] A. Sancar, "Structure and function of dna photolyase," *Biochemistry*, vol. 33, no. 1, pp. 2–9, 1994.

[43] A. Sancar, "Structure and function of dna photolyase and cryptochrome blue-light photoreceptors," *Chemical Reviews*, vol. 103, no. 6, pp. 2203–2238, 2003.

[44] A. Möller, S. Sagasser, W. Wiltschko, and B. Schierwater, "Retinal cryptochrome in a migratory passerine bird: a possible transducer for the avian magnetic compass," *Naturwissenschaften*, vol. 91, no. 12, pp. 585–588, 2004.

[45] M. Liedvogel and H. Mouritsen, "Cryptochromesa potential magnetoreceptor: what do we know and what do we want to know?," *Journal of the Royal Society Interface*, vol. 7, no. suppl_2, pp. S147–S162, 2009.

[46] C. Nießner, S. Denzau, J. C. Gross, L. Peichl, H.-J. Bischof, G. Fleissner, W. Wiltschko, and R. Wiltschko, "Avian ultraviolet/violet cones identified as probable magnetoreceptors," *PLoS ONE*, vol. 6, no. 5, p. e20091, 2011.

[47] A. Lukacs, A. P. Eker, M. Byrdin, K. Brettel, and M. H. Vos, "Electron hopping through the 15 å triple tryptophan molecular wire in dna photolyase occurs within 30 ps," *Journal of the American Chemical Society*, vol. 130, no. 44, pp. 14394–14395, 2008.

[48] B. D. Zoltowski, A. T. Vaidya, D. Top, J. Widom, M. W. Young, and B. R. Crane, "Structure of full-length drosophila cryptochrome," *Nature*, vol. 480, no. 7377, p. 396, 2011.

[49] M. Murakami, K. Maeda, and T. Arai, "Structure and kinetics of the intermediate biradicals generated from intramolecular electron transfer reaction of FAD studied by an action spectrum of the magnetic field effect," *Chemical Physics Letters*, vol. 362, no. 1-2, pp. 123–129, 2002.

[50] K. Maeda, S. R. Neil, K. B. Henbest, S. Weber, E. Schleicher, P. J. Hore, S. R. Mackenzie, and C. R. Timmel, "Following radical pair reactions in solution: a step change in sensitivity using cavity ring-down detection," *Journal of the American Chemical Society*, vol. 133, no. 44, pp. 17807–17815, 2011.

[51] K. Maeda, A. J. Robinson, K. B. Henbest, H. J. Hogben, T. Biskup, M. Ahmad, E. Schleicher, S. Weber, C. R. Timmel, and P. Hore, "Magnetically sensitive light-induced reactions in cryptochrome are consistent with its proposed role as a magnetoreceptor," *Proceedings of the National Academy of Sciences*, vol. 109, no. 13, pp. 4774–4779, 2012.

[52] D. M. Sheppard, J. Li, K. B. Henbest, S. R. Neil, K. Maeda, J. Storey, E. Schleicher, T. Biskup, R. Rodriguez, S. Weber, *et al.*, "Millitesla magnetic field effects on the photocycle of an animal cryptochrome," *Scientific Reports*, vol. 7, p. 42228, 2017.

[53] J. J. Sakurai, "Quantum mechanics," 1994.

[54] M. I. Eides and T. J. Martin, "Universality of leading relativistic corrections to bound state gyromagnetic ratios," in *Gribov-80 Memorial Volume: Quantum Chromodynamics and Beyond*, pp. 401–412, World Scientific, 2011.

[55] J. R. Lakowicz, *Principles of fluorescence spectroscopy*. Springer Science & Business Media, 2013.

[56] S. R. Neil, K. Maeda, K. B. Henbest, M. Goez, R. Hemmens, C. R. Timmel, and S. R. Mackenzie, "Cavity enhanced detection methods for probing the dynamics of spin correlated radical pairs in solution," *Molecular Physics*, vol. 108, no. 7-9, pp. 993–1003, 2010.

[57] C. A. Dodson, C. J. Wedge, M. Murakami, K. Maeda, M. I. Wallace, and P. J. Hore, "Fluorescence-detected magnetic field effects on radical pair reactions from femtolitre volumes," *Chemical Communications*, vol. 51, no. 38, pp. 8023–8026, 2015.

[58] L. M. Antill and J. R. Woodward, "Flavin adenine dinucleotide photochemistry is magnetic field sensitive at physiological ph," *The Journal of Physical Chemistry Letters*, vol. 9, no. 10, pp. 2691–2696, 2018.

[59] K. B. Henbest, K. Maeda, P. J. Hore, M. Joshi, A. Bacher, R. Bittl, S. Weber, C. R. Timmel, and E. Schleicher, "Magnetic-field effect on the photoactivation reaction of Escherichia coli DNA photolyase," *Proceedings of the National Academy of Sciences*, vol. 105, no. 38, pp. 14395–14399, 2008.

[60] D. M. Sheppard, *Cavity Enhanced Detection of Biologically Relevant Magnetic Field Effects*. PhD thesis, 2016.

[61] D. Zhong, "Electron transfer mechanisms of dna repair by photolyase," *Annual Review of Physical Chemistry*, vol. 66, pp. 691–715, 2015.

[62] C. Bialas, L. E. Jarocha, K. B. Henbest, T. M. Zollitsch, G. Kodali, C. R. Timmel, S. R. Mackenzie, P. L. Dutton, C. C. Moser, and P. Hore, "Engineering an artificial flavoprotein magnetosensor," *Journal of the American Chemical Society*, vol. 138, no. 51, pp. 16584–16587, 2016.

[63] C. Bialas, D. Barnard, D. Auman, R. McBride, L. Jarocha, P. J. Hore, P. L. Dutton, R. Stanley, and C. C. Moser, "Ultrafast flavin/tryptophan radical pair kinetics in a magnetically sensitive artificial protein," *Physical Chemistry Chemical Physics*, 2019.

[64] J. R. Lakowicz, *Principles of Fluorescence Spectroscopy; 3rd edition; Springer, New York,*. 2006.

[65] M. Brinkley, "A Brief Survey of Methods for Preparing Protein Conjugates with Dyes, Haptens and Crosslinking Reagents," *Bioconjugate Chemistry*, vol. 3, no. 1, pp. 2–13, 1992.

[66] T. S. Pierce, "Crosslinking technical handbook," *Thermo Fisher Scientific, Rockford, IL, USA*, 2009.

Appendices

Appendix A

MAGNAPULSA

MagnaPulsa is a home-built magnetic pulse produces. It is driven by a microprocessor and supplied DC power externally. The period and duty cycle of the pulses can be adjusted by the user, and signal is triggered by a button.

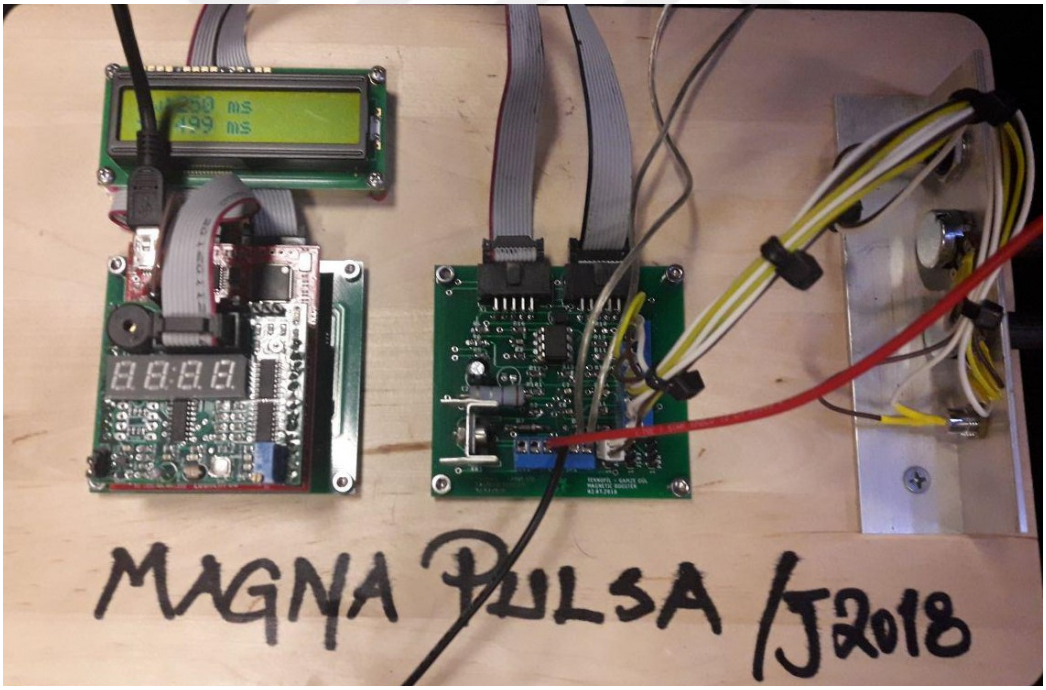

Figure A.1: Internal design of our home-built magnetic pulse producer

MagnaPulsa has a very short rising and falling time in the μs range which is important for the magnetoreception experiments because the lifetime of states are in this range.

MagnaPulsa send signals to the electromagnet which is made of a solenoid wounded on a ferrite core.

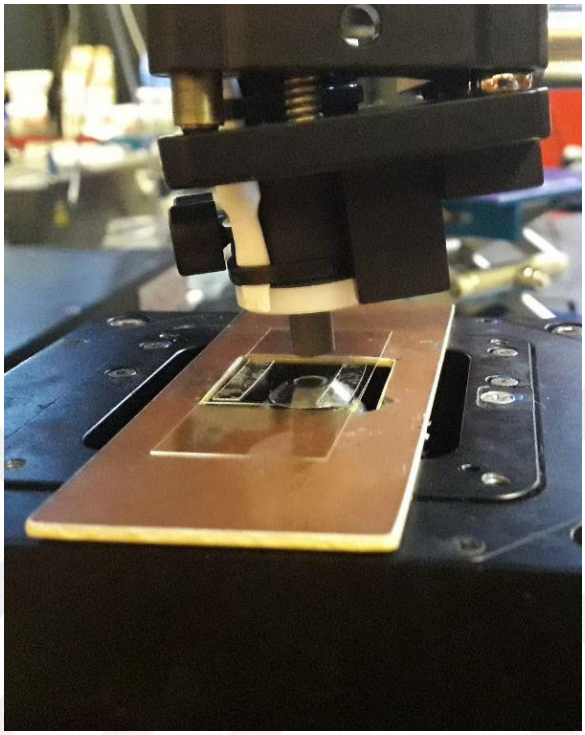

Figure A.2: Solenoid of MagnaPulsa wounded over a ferrite core

The solenoid is placed on to the sample holder with a translational stage. The stage also adjust the magnetic field strength by moving the solenoid in vertical direction. The maximum magnetic field is generated by MagnaPulsa is 35 mT (T = 500 ms Duty.C = 50%) when the supply voltage and current are optimum for operation.

Appendix B

MAGNETIC FIELD EFFECT CALCULATION

Magnetic field is calculated according to Equation 4.1; however, several noise components affect its credibility. Therefore, the following algorithm is developed to obtain an average magnetic field through the experiments.

Figure B.1 shown one run of the experiment which is approximately 10 seconds. We ignore the first 2-3 period of magnetic field because photobeaching dominates that region. Starting around t = 3 s, we calculate the magnetic field effect in each period and take the average over N period.

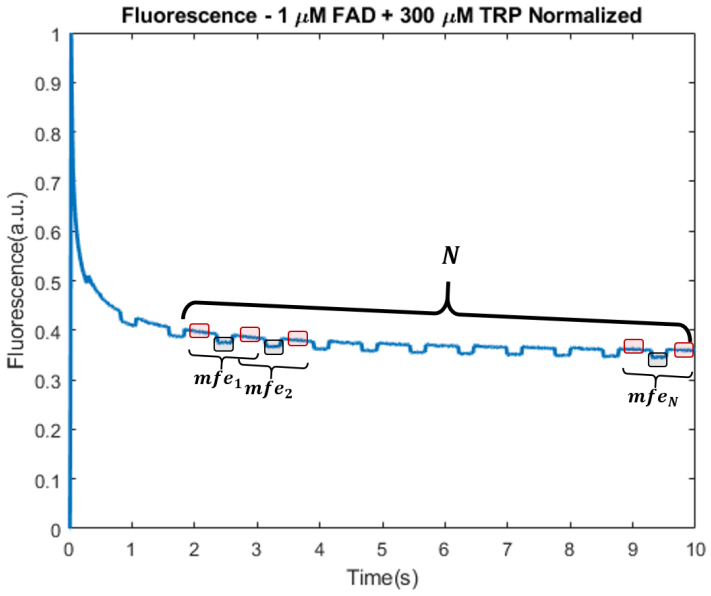

Figure B.1: Average magnetic field effect over N periods

The calculation of magnetic field effect for each period is also affected by the photobleaching. Therefore, we average the region shown with red boxes in Figure B.2, and obtain F(0) data.

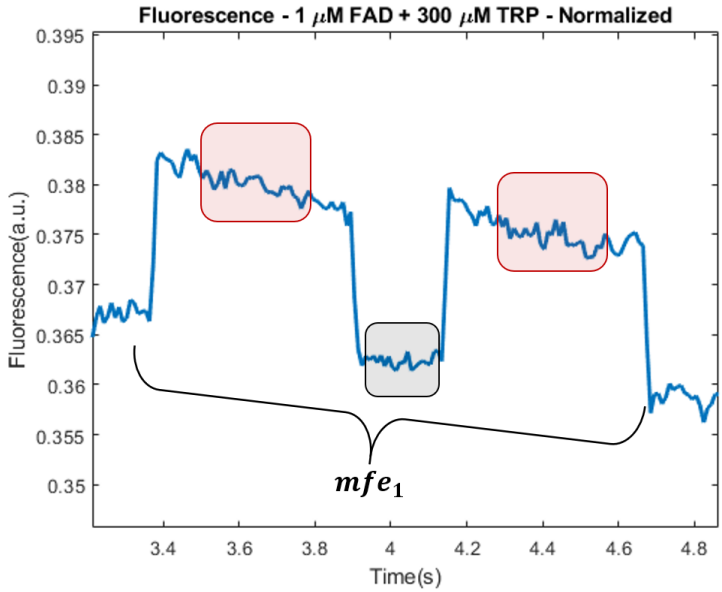

Figure B.2: Magnetic field effect for one period

Then, we take the average of the data point in blue box as F(B) data and calculate the normalized magnetic field effect as follows:

$$mfe_1 = \frac{F(B) - F(0)}{F(0)} \tag{B.1}$$

and average normalized magnetic field:

$$mfe = \frac{\Sigma mfe_i}{N} \tag{B.2}$$

We repeat the calculation for each repetition of the experiment, and take their average and standard deviation for credible results.

Appendix C

DATA PROCESSING

C.0.1 Total Fluorescence Calculation

```
clc
clear all
Files=dir('*.tif');

% Variables
number_of_frames = 2800;
fps = 100;
% Initializations
total_intensity_array = zeros(length(Files),number_of_frames);
norm_total_intensity_array = zeros(length(Files),number_of_frames);
total_average = zeros(length(Files),1);
total_average_bleaching = zeros(length(Files),1);

% Read the images and find total fluorescent for each image
for k=1:length(Files)
for i=1:number_of_frames
image(:,:,i)=imread(Files(k).name,i);
end

for j=1:number_of_frames
summation(1,:,j)=sum(image(:,:,j));
total_intensity(:,j) = sum(summation(1,:,j),2);
end
total_intensity_array(k,:) = total_intensity;
norm_total_intensity_array(k,:) = (total_intensity-total_intensity(1))...
/(max(total_intensity-total_intensity(1)));

total_average(k,1) = sum(total_intensity)/length(total_intensity)...
/max(total_average(k,1));
total_average_bleaching(k,1) = sum(total_intensity(end-50:end))...
/length(total_intensity(end-50:end));
end
```

```
t = linspace(0,number_of_frames/fps, length(total_intensity));

% Intensity Plots
figure
for i= 1:length(Files)
plot(t,total_intensity_array(i,:))
hold on
end
xlabel('Time(s)')
ylabel('Fluorescence')
title('Fluorescence - FAD+TRP')
legend(Files.name)
hold off

figure
for i= 1:length(Files)
plot(t,(total_intensity_array(i,:)-total_intensity_array(i,1))...
/max(total_intensity_array(i,:)-total_intensity_array(i,1)))
hold on
end
xlabel('Time(s)')
ylabel('Fluorescence')
title('Fluorescence - FAD+TRP Normalized')
legend(Files.name)
hold off

figure
for i= 1:length(Files)
plot(smooth(norm_total_intensity_array(i,:))
hold on
end
xlabel('Time(s)')
ylabel('Fluorescence')
title('Fluorescence - FAD+TRP Normalized')
legend(Files.name)
hold off
```

C.0.2 Fast Fourier Transform

```
for i = 1:length(Files)
a = total_intensity_array(i,:);
% figure
% plot(a)
% title(Files(i).name)
a = a(1500:end-100);
```

```
t_a = t(1:length(a));
L = length(a);
Fs = ones(length(Files),1)*100;
fit_eq_a = fit(t_a',a','exp2')

f_a = fit_eq_a.a*exp(fit_eq_a.b *t_a) +fit_eq_a.c*exp(fit_eq_a.d*t_a);

noise_a = a -f_a;

figure
plot(t_a,a)
hold on
plot(t_a,f_a,'r')
hold on
plot(t_a,noise_a,'g')
xlabel('Time(s)')
ylabel('Fluorescence')
title(Files(i).name)
legend('Original','2-Exponential Fit','Noise')

fft_noise_a = fft(noise_a);

fft_a = abs(fft_noise_a/L);
fft_a = fft_a(1:L/2+1);
fft_a(2:end-1) = 2*fft_a(2:end-1);
f = Fs(i)*(0:(L/2))/L;

[all_pks,locs] = findpeaks(fft_a)
figure
plot(f,fft_a)
findpeaks(fft_a,f,'Threshold',mean(all_pks))
xlabel('f (Hz)')
ylabel('|Data(f)|')
[pks, location]=findpeaks(fft_a,f,'Threshold',mean(all_pks));
text(location,pks,num2str(location', '%.3f'))
title(Files(i).name)
end
```

C.0.3 MFE Calculation

```
for i= 1:length(Files)
figure
plot(smooth((total_intensity_array(i,:)-total_intensity_array(i,1))...
/max(total_intensity_array(i,:)-total_intensity_array(i,1))))
xlabel('Time(s)')
```

```
ylabel('Fluorescence')
title(Files(i).name)
Files(i).name
initial(i) = total_intensity_array(i,4);
final(i) = total_intensity_array(i,500);
end

close1 = 0;
close2 = 0;
close_total = 0;
open = 0;
mfe = 0;
total_period = 85;
close_period = 50;
number_of_data=10;
delay = 5;
a = smooth(norm_total_intensity_array(1,:));
first_high_point = 412; %must be determined by us
a = a(first_high_point:end);
plot(a)
mfe=0;
for g = 0:2
close1 = mean(a((g*total_period)+delay:(g*total_period)+number_of_data+delay))
close2 = mean(a(((g+1)*total_period)+delay:((g+1)*total_period)+number_of_data+delay))
close_total = (close1+close2)/2
open = mean(a(((g*total_period)+close_period+delay):((g*total_period)...
+number_of_data+close_period+delay)))
(g*total_period)+close_period+delay:((g*total_period)...
+number_of_data+close_period+delay)
mfe(g+1) = -((close_total-open)/close_total)*100
end
mfe_array(1)= mean(mfe)
```